

The Third Intron of IRF-8 Restricts Its Expression in Non-Hematopoietic Cells in Concert with MafK to Elicit Repressive Chromatin

Nitsan Fourier^{1¶}, Mamduh Khateb^{1¶}, Ofer Barnea-Yizhar^{1¶}, Sigal Ram¹, Ulfert Rand², Hansjörg Hauser², Donato Tedesco³, Manabu Nakayama⁴, Aviva AAzriel¹, and **Ben-Zion Levi**^{1*}

¹Department of Biotechnology and Food Engineering, Technion - Israel Institute of Technology, Haifa, Israel

²Department of Gene Regulation and Differentiation, Helmholtz Centre for Infection Research, Braunschweig, Germany,

³Cellecta, Inc., Mountain View, California, United States of America,

⁴Laboratory of Pharmacogenomics, Graduate School of Pharmaceutical Sciences, Chiba University, Chiba, Japan

*Corresponding author, E-mail: blevi@technion.ac.il

¶These authors contributed equally to this work.

Abstract

Interferon Regulatory Factor-8 (IRF-8) serves as a key factor in the hierarchical differentiation towards monocyte/dendritic cell lineages. IRF-8 is also a tumor suppressor gene that is repressed mainly in myeloid leukemias. Insights to molecular mechanisms essential for its hematopoietic specific expression are documented. However, the molecular mechanisms restricting IRF-8 expression in non-hematopoietic cells are not elucidated. Collectively, chromatin organization and architecture governs gene expression; "active chromatin" is accessible to the transcriptional machinery and conversely, "repressed chromatin" leads to gene repression. Here we show that the repression of IRF-8 expression in restrictive cells is mediated by its 3rd intron. Removal of this intron alleviates the repression of BAC IRF-8 reporter gene in these cells. Fine deletion analysis point to conserved regions within this intron mediating its restricted expression. Further, this intron alone initiates gene silencing only in expression-restrictive cells when cloned near a reporter gene in a retroviral vector, pointing to its possible role as initiator of repressed chromatin state. Additionally, histone Post-Translational Modifications (PTMs) analysis points to the role of chromatin remodeling in active repression of IRF-8 expression in restrictive cells. MafK was identified by barcoded shRNA library screen as a candidate gene to orchestrate chromatin dynamic changes in IRF-8 restrictive cells. MafK binds *in-vitro* to the 3rd intron and *in-vivo* to the IRF-8 locus in expression-restrictive cells. MafK inhibition in these cells led to significant enhancement of IRF-8 expression. Collectively, our results point to the role of IRF-8 3rd intron as a "nucleation core" for chromatin condensation eventually leading to the repression of the entire IRF-8 locus.

Introduction

Bone marrow derived hematopoietic stem cells (HSC) give rise to lineage specific progenitors among which is the Common Myeloid Progenitor (CMP) cell that can further differentiate to Granulocyte\Monocyte Progenitor (GMP). The latter is the source for three subsets of myeloid cells; granulocytes, dendritic cells (DCs) and monocytes. Transcription factors play key roles in this differentiation process through the regulation of a characteristic set of lineage-specific target genes (1-4).

Interferon Regulatory Factor -8 (IRF-8) is a nuclear transcription factor that belongs to the IRF family and is constitutively expressed in the hematopoietic lineages of monocyte/macrophage cells, DCs, B-cells and at low levels in resting T-cells (5, 6). IRF-8 serves as a key factor in the hierarchical differentiation from HSC towards the monocyte\DC lineages. Expression of IRF-8 can be further induced in these cells by IFN- γ (7). Mice with IRF-8 null mutation are defective in the ability of myeloid progenitor cells to mature towards monocyte\DC lineages. These KO mice eventually develop chronic myelogenous leukemia (CML) like syndrome (8). Together, these observations highlight the role for IRF-8 in myelopoiesis and as a tumor suppressor gene of myelo-leukemias such as CML.

In an attempt to identify the molecular mechanisms leading to this lineage restricted expression of IRF-8, we employed IRF-8 Bacterial Artificial Chromosome (BAC) reporter constructs. Such BAC constructs harbor all the regulatory regions as well as the *cis* and distal elements that define expression domains of a gene of interest such as scaffold/matrix attachment regions that isolate the gene from distal regulation (9). Using successive deletion strategy, we demonstrate that the 3rd intron of IRF-8 harbors regulatory elements that suppress its expression in restrictive cells. We provide evidence showing that changes in chromatin architecture, e.g. nucleosome occupancy

and histone post-translational modifications (PTM) profile, are mediators of active suppression of IRF-8 expression in restrictive cells. Cloning of IRF-8 3rd intron near a reporter gene in a retroviral vector results in gene silencing only in restrictive cells, pointing to its role as nucleation core for chromatin condensation when the virus assembles chromatin conformation upon integration. Interestingly, barcoded shRNA library screen revealed that MafK mediates, in part, IRF-8 repression in restrictive cells by affecting the chromatin state.

Materials and Methods

Cell lines

NIH3T3 (Mouse embryo fibroblast), RAW (RAW267.4, Murine monocytes/macrophages-like) and 293FT were obtained from ATCC, Manassas, Virginia, USA (CRL-1658, TIB-71 and CRL-3216, respectively). All cell lines were maintained in DMEM supplemented with 10% Fetal Calf Serum, 2.5 µg/ml Amphotericin and 50 µg/ml Gentamycin Sulfate (Biological Industries, Beit-Haemek, Israel).

Animals

C57BL/6J (Harlan Biotech, Rehovot, Israel) mice were maintained in microisolator cages in a viral pathogen-free facility. All animal works conformed to the guidelines of the animal care and use committee of the Technion.

Cell preparation and culture of BMDM and GMP

Bone marrow derived macrophages (BMDMs) – Bone marrow cells were isolated from femurs and tibias of 6-8 weeks old C57BL/6J females and cultured in DMEM supplemented with 30% CCL1 cell culture supernatant (source for M-CSF), 20% Fetal Calf Serum, 2.5 µg/ml Amphotericin and 50 µg/ml Gentamycin Sulfate. After 7 days of cultivation, typical BMDMs were obtained.

GMPs– Bone marrow cells were isolated as described above and grown in DMEM supplemented with 10% Fetal Calf Serum, 10% filtered WEHI condition media (a source for IL-3), 10 ng/ml recombinant mouse stem cell factor (rmSCF) (Peprotech, Rocky Hill, NJ, USA), 2.5 µg/ml Amphotericin and 50 µg/ml Gentamycin Sulfate. After 7 days of cultivation, non-adherent cells were collected.

BMDM and GMP cells phenotype was verified by flow cytometry with anti-CD34 antibody and qRT-PCR with specific primers targeting cell type-specific genes, such as CD34, Tie2 (GMP) and M-CSF receptor (BMDM). Characterization of mouse BM derived GMP and BMDM cells is detailed in supplemental S1A Fig. 90% of the progenitor cell population were CD34^{high} and exhibited high mRNA levels of the progenitors-associated genes CD34 and Tie2 (supplemental S1SB Fig. and S1C Fig., respectively) compared to mature BMDM. On the other hand, BMDM exhibited relatively high expression level of the macrophage-associated gene, M-CSF receptor (supplemental S1D Fig.). GMPs in contrast to BMDM were restrictive for IRF-8 expression and were not responsive to IFN- γ induction (supplemental S1E Fig.).

BAC IRF-8 reporter constructs

The BAC clone 7H10 was obtained from the BACPAC Resource Center, Children's Hospital Oakland Research Institute, Oakland, California, USA. This BAC clone harbors 219,907bp encompassing the murine IRF-8 locus as described hereafter. Construction of the various BAC-IRF8 reporter constructs was generated using the Red ET cloning procedures (10) as outlined in the text. In principal, a reporter cassette containing a reporter gene open reading frame followed by Neo resistance gene placed under the control of dual promoters, phosphoglycerate kinase promoter (PGK) and SV40 early enhancer/promoter region, conferring Neo resistance gene expression in *E.coli* and mammalian cells, respectively, was generated by PCR and cloned to pSK plasmid. The reporter cassette was amplified by PCR with two primers harboring 50bp homologous arms to the site of integration. Homologous recombination was performed by the recombination proteins of bacteriophage lambda (ET recombination) (10). The exact integration of the reporter cassette for each BAC IRF-8 construct was verified by DNA sequence.

Generating BAC IRF-8 reporter construct stable clones

7×10^5 cells of either RAW or NIH3T3 cells were seeded in 6 wells tissue culture plates with 2 ml of fresh DMEM medium containing 5% FCS. 18 hrs later, cells were transfected with $6 \mu\text{g}$ of the DNA corresponding to the various BAC IRF-8 reporter constructs using Metafectene Pro according to the manufacturer's protocol (Biontext laboratories GmbH, Germany). Cells were harvested 24 hrs later and plated on 10 cm culture dishes and after additional 16 hrs, Geneticin (G418) was added to select for stably transfected clones. Individual clones were isolated about 14-18 days later, and the copy number of various transfected BAC IRF-8 reporter constructs was determined by qPCR of isolated genomic DNA in comparison to endogenous single copy genes such as IRF-8 and GAPDH. Additionally, PCR using genomic DNA as template was performed with 10 primer sets spanning along the BAC IRF-8 reporter construct to verify that the whole BAC IRF-8 reporter construct was integrated.

Deletions using VCre recombination system

Since our BAC constructs harbor both classical Cre/loxP as well as FLP-FRT site specific recombination systems, we turned to a newly described system utilizing new site-specific recombination system, VCre/VLoxP (11). Using recombineering approach as described above, new BAC constructs, in which the IRF-8 3rd intron or three evolutionary Conserved Non-coding Sequences (CNS, Fig. 2) were flanked by two VLoxP sites, were generated by PCR. VCre recombinase was sub-cloned from pTurboVCre (11) to pMSCV Puromycine (Puro) retroviral vector. The VCre constructs were transfected to restrictive NIH3T3 cells and numerous clones were collected. To perform 3rd intron deletion within the cells, clones were transduced with either empty retroviral vector or retroviral vector encoding for the VCre gene. Subsequently, the reporter gene expression was analyzed.

Formaldehyde Assisted Isolation of Regulatory Elements (FAIRE)

The protocol was adopted from Simon and Giresi (12). Briefly, cells were grown to 80-90% confluence, harvested, cross-linked with 1% formaldehyde (5 min for RAW cells and 15 min for NIH3T3 cells), lysed, chromatin was isolated and aliquot to INPUT and FAIRE DNA samples. FAIRE DNA samples were subjected to phenol/chloroform extraction; the nucleosome depleted DNA phase (aqueous phase) was retrieved, de-crosslinked and taken for analysis. The INPUT sample was first de-crosslinked and only then subjected to phenol/chloroform extraction. Equal amount of purified DNA of both INPUT and FAIRE samples were used as templates for qPCR (INPUT is set as reference). qPCR was performed with 18 sets of primers pairs generating PCR fragments covering with partial overlaps tilling the entire length of the IRF-8 3rd intron (see Fig. 3 and Supplemental Table 1). Enrichment levels of nucleosome depleted DNA, between the FAIRE and INPUT samples were calculated for designated locations (PCR segment) across the IRF-8 3rd intron.

Fast Chromatin Immuno-precipitation (Fast-ChIP)

The protocol was adopted from Nelson et al. (13). Briefly, cells were crosslinked with formaldehyde; DNA was then extracted, fragmented and precipitated using monoclonal antibodies recognizing specific histone PTMs. Three histone PTMs were analyzed- α H3K27ac (ab4729, abcam), α H3K4me2 (17-677, upstate), α H3K27me3 (17-622, upstate), anti-normal mouse IgG (ChIPAb and kit, upstate) and anti-normal rabbit IgG (ChIPAb and kit, upstate). Following IP the sample was de-crosslinked and DNA purified. The enriched de-crosslinked DNA samples were subjected to qPCR with 18 sets of primers pairs described under FAIRE. This resulted in the Fold of Enrichment (FoE) for a specific cell type, with a specific antibody over a designated location (PCR

segment) across the IRF-8 3rd intron. The ChIP results are presented as Fold of Difference (FD), which is the ratio of the FoE values between every two cell types analyzed.

Real Time PCR

The primers used for real-time PCR for EZH2, IRF-8, IRF-1 and GAPDH were designed using PrimerExpress™ software (Applied Biosystems, Foster City, California, USA) (see Supplemental Table 1). Primers for Tie2 and CD34 were described previously (14, 15). One µg of total RNA was reverse transcribed to cDNA using High Capacity cDNA Reverse Transcriptase kit (Ambion, Austin, Texas, USA) according to the manufacturer's protocol. cDNA was amplified with two primers for each gene using Power SYBR Green PCR Master Mix (Applied Biosystems) and Applied Biosystems 7300 real-time PCR System according to the manufacturer's instructions. The amplification reaction condition was 95C for 15 min followed by 40 cycles of 95C for 10 s, 60C for 20 s and 72C for 15 s. The estimated amount of transcripts was normalized to GAPDH mRNA expression. The data is presented as the relative expression of the gene of interest compared with GAPDH.

Electrophoretic Mobility Shift Assay (EMSA)

Three to six µg nuclear extract from NIH3T3 and RAW cells were incubated with approximately 40,000 cpm of labeled probe corresponding to mouse IRF-8 3rd intron

CNS-3 (sense 5 -
AGCGAGGACGCTCACTACTCCCGTTTCCTTAATTCAGCATTTTAAGA-3 and
antisense 5-
TCTTAAAATGCTGAATTAAGGAAACGGGAGTAGTGAGCGTCCTCGCT-3).

The EMSA reaction was performed in binding buffer (50 mM HEPES (pH 7.9), 25 mM MgCl₂, 259 mM KCl, 0.025% bromophenol blue, 0.025% xylene cyanole, 10% Ficoll, 3% glycerol and 1 μg polyd(IC)) for 20 minutes in RT. For competition assay 5-20 fold excess of probes containing WT or mutated MafK binding site (sense 5-CTCCCGTTTCCTTAATTCGTACTTTTAAAGA-3, and antisense 5-TCTTAAAGTACGAAATTAAGGAAACGGGAG-3) were used. Samples were loaded on a pre-run 7% polyacrylamide gel and run at 170V for 3 hrs. Dried gels were subsequently subjected to autoradiography.

shRNA library screen

The Decipher murine pooled Lentiviral shRNA library module 1 obtained from Cellesta, Inc. (Mountain View, California, USA), targeting signaling pathways (TFs and chromatin modifiers are included) was employed (16). The target cell line NIH3T3 harboring BAC-IRF-8.1 was infected in three replicates with Lentiviral particles at a multiplicity of infection of 0.7. Positively infected cells were selected with Puromycin for 72 hrs. Each replicate was subjected to fluorescence-activated cell sorting (FACS) for the enrichment of the top 5% fluorescent cells and low 50% fluorescent cells as control. We reasoned that knocking-down one of the possible repressive factors will result in alleviation of IRF-8 repression on expression, leading to the subsequent expression of the fluorescent reporter gene. To identify the enriched shRNAs, genomic DNA was extracted from each cell population and following two rounds of PCR amplification subjected to Next Generation Sequencing (NGS) (HiSeq, Illumina, San Diego, California, USA) according to the library accompanying protocol (16). The sequencing data was analyzed using the special statistical tools provided with the Decipher library (16). The 10 top hit list contained genes (shRNAs) that were enriched

by at least two fold against background with at least two different gene specific shRNAs.

Lentiviral shRNA transduction

For shRNA library screen validation shRNA targeting MafK was sub-cloned into pLKO.1-TRC cloning vector (a gift from David Root, plasmid # 10878, Addgene, Cambridge, Massachusetts, USA) according to Addgene's pLKO.1 protocol. Briefly, pLKO.1-TRC was digested with AgeI and EcoRI and 7kb fragment was gel-purified. Double-strand DNA oligonucleotides were designed according to the sequence of the most enriched MafK construct from the barcoded shRNA library with appropriate overhangs for ligation with pLKO.1-TRC digested fragment. For lentiviral transduction, 293T cells were transiently transfected with lentiviral vector and pMDG and psPAX2 (a gift from Didier Trono, plasmid # 12260, Addgene, Cambridge, Massachusetts, USA) packaging plasmids using Lipofectamine 2000 (Life Technologies, Grand Island, New-York, USA) in accordance with manufacturer's protocol. Lentiviral supernatant was collected 48 hrs post transfection. NIH3T3 harboring BAC IRF-8.1 construct were transduced with lentiviral supernatant and 8 ug/ml polybrene. Transduced cells were selected with 3 ug/ml Puromycin.

Luciferase reporter assay

Plasmid reporter constructs – these constructs were generated by PCR amplifying the IRF-8 3rd intron and the GAPDH 2nd intron (1720bp) with primer flanked by Mlu I site (Int3 5'- GCTTAACGCGTGTA ACTATCTGTTGGGACC; 3' GCTATACGCGTCTATGGGAAAGGGGACAGAC; and GAPDH 5'- GCTTAACGCGTGGATCCGGATGAGGTGGCCGAAGCGC; 3'- GCTATACGCGTGGATCCACTCCTCATGGGTCTGTAGT) and sub-cloned to

pGL3 luciferase vector (pGL3-Luc) driven by the Nramp promoter (-1555, detailed in (17)). The Mlu I site is upstream the Nramp promoter generating pGL3-Luc-int3 and pGL3-Luc-GAPDHint2. These plasmids were transfected to NIH3T3 cells and reporter gene assays were performed exactly as previously described (17).

Retroviral reporter construct - the retroviral luciferase reporter constructs were generated by PCR amplifying the pGL3 reporter cassettes described above and sub-cloning into the Mlu I site the pMSCV retroviral vector, generating pMSCV-Luc, pMSCV-Luc-int3, pMSCV-Luc-GAPDHint2, respectively. NIH3T3 cells were infected and reporter gene assay were performed 72 hrs later (to ensure chromosomal integration) as described above. Retroviral titers were determined by the QuickTiter™ Retrovirus Quantitation Kit according to the manufacturer protocol (Cell-Biolabs Inc. San Diego, California, USA).

AdOx treatment

NIH3T3 cells harboring BAC-IRF-8.1 construct were plated 24 hrs prior to AdOx (A7154, Sigma-Aldrich) treatment. Cells were either untreated or treated with 25 μ M AdOx. 72 hrs post-treatment EGFP and IRF-8 expression were analyzed using flow cytometry as described hereafter.

Flow cytometry

NIH3T3 cells harboring BAC IRF-8.1 were infected with lentiviral particles containing shRNA targeting MafK or empty vector. Following antibiotic selection, flow cytometry analysis was performed using BD LSR-II flow cytometer (BD Bioscience, San Jose, California, USA) and data was analyzed using Flowing Software 2 (Cell Imaging Core, Turku Centre for Biotechnology). Goat anti-IRF-8 (C-19) and donkey anti-goat IgG

(CFL405) were purchased from Santa Cruz Biotechnology. Cells were fixed in 4% paraformaldehyde, permeabilized with 0.5% saponin, blocked with 10% normal donkey serum (D9663, Sigma) and stained with anti-IRF-8 (1:100 dilution) and anti-goat IgG (1:100 dilution) or with anti-goat IgG alone as control. Unstained wild-type NIH3T3 cells were used as negative control for EGFP.

Results

The third intron of IRF-8 harbors a lineage restricting regulatory element

In an attempt to identify the molecular mechanisms leading to IRF-8 repression in restrictive cells we employed Bacterial Artificial Chromosome transgenesis (9, 18). BAC harbors all the regulatory regions as well as the *cis*-elements and regains original chromatin architecture in a given cell or tissue allowing for authentic expression of a gene of interest regardless of integration point (9, 19). To generate IRF-8 BAC reporter constructs, we used the BAC genomic clone 7H10 that is 219,907bp long harboring the entire murine IRF-8 gene (20,319bp) and additional upstream sequence of 118,857bp and downstream sequence of 80,731bp. Two BAC-IRF-8 reporter constructs were initially generated by inserting a reporter cassette containing a fluorescent reporter gene and an independently transcribed selectable marker (see schematic illustrations in Fig. 1). In the first construct, BAC-IRF-8.1, the reporter gene cassette was inserted at the translation start site of IRF-8, and in the second construct, BAC-IRF-8.2, the whole IRF-8 coding region from translation start site to the stop codon was replaced with the reporter cassette. These two BAC-IRF-8 reporter constructs were transfected either to IRF-8 hematopoietic permissive cell line, the macrophage cell line RAW, or to non-hematopoietic restrictive fibroblast cell line NIH3T3. In general, at least 10 clones harboring the various BAC-IRF-8 constructs were selected and the copy number was determined by quantitative PCR. In each tested group, at least 5 clones harbored 1-2 integrated BAC copies and the rest incorporated up to 20 copies. In all similar assays reported hereafter, linear differences in fluoresces output were observed in direct correlation to the copy number of integrated BACs. Fluorescence of the reporter gene before and following exposure to IFN- γ was visualized under fluorescent microscope.

In addition, RNA was extracted from the cells and relative mRNA levels of the reporter gene and the endogenous IRF-8 gene were determined by qRT-PCR. For the sake of simplicity, the data presented in the relevant figures hereafter is of a single representative clone harboring 1-2 copies of integrated BAC. It is clear from Fig. 1A that in IRF-8 permissive cells, RAW macrophage cell line, both the BAC driven reporter gene and the endogenous IRF-8 were induced by IFN- γ following transfection of the BAC-IRF-8.1 reporter construct (Fig. 1Ai and Fig.1Aii, respectively). Similarly, IRF-8 and the reporter gene were induced in macrophage cells transfected with the BAC-IRF-8.2 construct (Fig. 1B). As expected, both the BAC-IRF-8.1 driven reporter gene and the endogenous IRF-8 were not expressed in the restrictive cell line NIH3T3 (Fig. 1Ai, lower panel, and Fig. 1Aii). Surprisingly, the reporter gene was expressed and further induced in response to IFN- γ stimulation in NIH3T3 cells transfected with the BAC-IRF-8.2 construct (Fig.1Bi, lower panel). In contrast, and as expected, the endogenous IRF-8 was not expressed at all in these cells (Fig. 1Bii, compare black columns). These results indicated that the BAC-IRF-8.1 reporter construct is authentically reporting on IRF-8 lineage restrictive expression in response to IFN- γ stimulation; fluorescent in permissive cells and dark in restrictive cells. Furthermore, it is clear that the restricted expression of the IRF-8 reporter in the BAC-IRF-8.2 in restrictive NIH3T3 was impaired when the coding region of IRF-8 was deleted; i.e. from the second to the ninth exon including intervening introns. These results point to a restricting regulatory element(s) in NIH3T3 cells confined to the coding segment of the IRF-8 locus. Since IRF-8 is highly conserved in mammals, we reasoned that this restricting element is located in intronic region. Comparative sequence analysis revealed that the 2nd and the 3rd introns harbor evolutionary conserved regions (Fig. 2). The non-coding first exon and subsequent intron were not deleted in both BAC-IRF-8

reporter constructs. Therefore, two additional BAC-IRF-8 reporter constructs were generated in which the second or the third introns were deleted, BAC-IRF-8.3 (Fig.1C) and BAC-IRF-8.4 (Fig.1D), respectively. Deletion of the 2nd intron did not affect the cell type specific repression of the reporter gene; i.e. expressed in response to IFN- γ in permissive RAW cells and not expressed at all in restrictive NIH3T3 cells (Fig 1Ci, compare upper and lower panels). However, when the 3rd intron was deleted in the BAC-IRF-8.4 construct (Fig. 1Di), it was clear that the reporter gene was expressed and further induced by IFN- γ in both RAW and NIH3T3 cells; thus recapitulating the expression pattern of the reporter gene in the BAC-IRF-8.2 construct in which the whole coding region was deleted. Taken together, these results suggest that the cell type repression element of IRF-8 is confined to the 3rd intron. Furthermore, it suggests that an active repression mechanism is governing IRF-8 repression in restrictive cells.

IRF-8 3rd intron serves as nucleation core for chromatin condensation in restrictive cells

The results described above concerning the importance of the 3rd intron (1730bp) for IRF-8 cell-type specific repression relied on the fact that the 3rd intron was deleted from the BAC construct prior to the transfection to NIH3T3 cells. In order to analyze the reporter gene expression in a single clone before and following removal of the 3rd intron, we constructed a new BAC reporter construct, BAC IRF8.1-VLoxP. Since our BAC constructs already contain both classical Cre/LoxP as well as FLP-FRT site specific recombination systems, we turned to a newly described system that utilizes new site-specific recombination system, VCre/VLoxP (11). In the new BAC construct, IRF-8 3rd intron is flanked by two VLoxP sites. This new construct was transfected to restrictive NIH3T3 cells and numerous clones were isolated. To perform 3rd intron

deletion within the cells, clones were transduced with either empty retroviral vector or retroviral vector encoding for the VCre gene (detailed under Materials and Methods), and GFP expression was subsequently analyzed. Surprisingly, despite the fact that the intron was removed in clones harboring BAC IRF8.1-VLoxP construct, no reporter expression was detected by flow cytometry (data not shown) or under fluorescent microscope, even following treatment with IFN- γ (Fig. 3A). We hypothesized that since the BAC construct was initially transfected with an intact 3rd intron the IRF-8 locus within this BAC construct already gained condensed chromatin architecture in the restrictive cells, followed by yet undefined "epigenetic memory". Therefore, the subsequent removal of the 3rd intron within the cells had no effect on the expression and had no effect on the architecture state of the repressed chromatin (Fig. 3A). Even ectopic expression of PU.1, essential for IRF-8 expression (20), had no effect (data not shown). Hence, we initially deleted the 3rd intron using the VCre in bacteria and subsequently transfected it to NIH3T3 cells. Stable clones were isolated and GFP expression was evaluated under fluorescent microscope before and following treatment with IFN- γ (Fig. 3B). It is clear that removal of the 3rd intron prior to its transfection led to the expression of the reporter gene in the restrictive cells. These results recapitulate our results summarized in Fig. 1D in which the 3rd intron had been swapped with antibiotic expression cassette prior to the transfection to cells. The difference between these two experiments is the fact that the 3rd intron was "surgically" removed and not swapped with a selectable marker cassette. Additionally, it pointed to the fact that removal of the 3rd intron within restricting cells was not sufficient to alleviate repression. The intron should be initially deleted and only then the "naked DNA" is transfected to the cells. Upon integration, chromatin structure is assembled but since the 3rd intron is missing, the open chromatin architecture enables accession of the

transcriptional machinery to this area, therefore cells are fluorescent. When "naked DNA" harboring the 3rd intron is present, it probably recruits the Polycomb-group (PcG) machinery leading to chromatin condensation making this area inaccessible to the transcriptional machinery. Therefore, removal of the 3rd intron in these cells is ineffective since the repression machinery is already "on" (for review (21)). Taken together, these results points to the possible role of IRF-8 3rd intron as nucleation core for chromatin condensation.

To further establish the role of IRF-8 3rd intron as nucleation core for repression of the IRF-8 locus, we have cloned it downstream to a luciferase reporter gene in the reporter plasmid pGL-3 and as a control, we also cloned the 1720bp of the 2nd intron of GAPDH. These three reporter plasmids (pGL3, pGL3-int3, pGL3-GAPDHint2, detailed under Materials and Methods) were transiently transfected to NIH3T3 cells. However, no significant differences in luciferase activities between these three reporter constructs were noted (data not shown). We reasoned that in these transient transfection assays, the plasmids do not assemble chromatin conformation. Therefore, the IRF-8 3rd intron and the GPAPDH 2nd intron were sub-cloned to a retroviral vector, pMSCV, upstream to the reporter gene as detailed under Materials and Methods. 72 hrs following transduction, to ensure chromosomal integration, the cells were harvested, luciferase assays were performed, and the data was calibrated against cell number (protein level) and retroviral infection efficiency (for details see Materials and Methods). The luciferase activity of the cells transduced with the retroviral vector, pMSCV-Luc-int3, harboring the reporter gene and the 3rd intron upstream to its coding sequence exhibited significant decrease in the reporter gene activity (~5 fold) in comparison to the two other viral vectors control; pMSCV-Luc, and pMSCV-Luc-GAPDHint2 (Fig. 4A). However, no significant inhibition of the reporter gene was noted with the same

retroviral vectors in the IRF-8 permissive macrophage cell line RAW (Fig. 4B). Interestingly, when antibiotic selection was applied on NIH3T3 cells to select for transduced cells, the efficiency of transduction of only pMSCV-Luc-int3 was sharply reduced while that of pMSCV-Luc and pMSCV-Luc-GAPDHint2 was similar. Consequently, the above-mentioned reporter assays (Fig.4) were performed 72 hrs after transduction, however, selection pressure was not applied to exclude this bias. This suggests that in addition to the luciferase gene, the antibiotic resistance gene was also subjected to chromatin condensation, which prevents its accessibility to the transcriptional machinery. Taken together, these results points to the ability of the 3rd intron to induce effective local gene silencing when the integrating viral vectors gained chromosomal conformation. This was not observed with the control retroviral vectors that were highly luminescent. Furthermore, since this retroviral vector almost randomly integrates along the genome, it points to the general ability of the 3rd intron to elicit repression and thus, further support our BAC-IRF-8 reporter studies described above.

Fine deletions performed within the IRF-8 3rd intron alleviated expression in restrictive cells

In an attempt to identify the regulatory element(s) within the IRF-8 3rd intron that recruit the epigenetic machinery leading to gene repression, fine deletions within the conserved regions were performed. As seen in Fig. 2, bioinformatics analysis of the 1730bp long 3rd intron, using ECR Browser (22), revealed three evolutionary conserved non-coding sequences (CNS): CNS1, 2 and 3. In each CNS there are one or two dense clusters harboring putative TF binding motifs (Genomatix Software Suite (MatInspector (23))). To create constructs with CNSs deletion, the same VCre mediated experimental procedure described above was employed. BAC-IRF-8.1 construct that harbors the

GFP cassette inserted to the first methionine of the IRF-8 gene was used to evaluate the effect of such fine deletions. Three different deletions encompassing the three CNSs were performed; deletions of CNS1 (position 1-284), CNS2 (position 680-860) and CNS3 (position 1230-1730). Following VCre mediated removal of the antibiotic cassette, the new BAC constructs were transfected to restrictive cells and stable clones were further characterized; 7 clones from deletion of CNS1, 9 clones from deletion of CNS2 and 7 clones from deletion of CNS3. The GFP fluorescence in each clone was evaluated by microscopy before and following induction with IFN- γ . As shown in Fig. 5, a representative clone harboring the CNS2 deletion (Fig. 5, mid panel) exhibited a significantly higher level of GFP expression in comparison to the other two deletions and almost comparable to the removal of the whole intron. In addition, deletion of CNS3 (Fig. 5, lower panel) exhibited mid-level GFP expression in comparison to the deletion of CNS1, that was quiet dim but not dark (Fig. 5, top panel). Therefore, the two conserved regions, middle (CNS2) and 3' (CNS3), are more prominent regulatory elements and may serve as anchor sites for DNA binding factors (DBFs) that recruit the epigenetic machinery and affect chromatin architecture resulting in IRF-8 repression in restrictive cells.

Nucleosome occupancy variability between IRF-8 expression permissive and restrictive cell lines

The BAC reporter results clearly indicated that the repression of IRF-8 expression in restrictive cells is mediated by its third intron. Removal of this intron from the reporter construct alleviated IRF-8 repression. In order to characterize the molecular mechanism governing this lineage specific restriction, we explored the involvement of chromatin architecture. Initially, differences in nucleosome occupancy over IRF-8 3rd intron between RAW and NIH3T3 cell lines was analyzed using formaldehyde-assisted

isolation of regulatory elements (FAIRE) technique (12). This is an alternative approach to nuclease hypersensitivity assay aimed at identifying DNA regulatory elements that are evicted of nucleosomes (for details see Materials and Methods (12)). The data in Fig. 6 is presented as Fold Difference (FD) ratio of nucleosome depleted DNA between the RAW and NIH3T3 cell lines across the entire IRF-8 3rd intron. The results clearly demonstrate that the 3rd intron is more depleted of nucleosomes in hematopoietic IRF-8 permissive cell line, RAW, in comparison to the non-hematopoietic cell line, NIH3T3 (Fig. 6). These results suggest that a loosely structured chromatin is present in IRF-8 permissive cells.

Repressive chromatin architecture is abundant over the IRF-8 3rd intron in expression restrictive cells

We next tested whether the difference in chromatin architecture between IRF-8 permissive and restrictive cells revealed by FAIRE is also supported by differential histone PTM profile. For that purpose, we compared histone 3 lysine 27 tri-methylation (H3K27me3), a modification correlated with dense chromatin architecture (24-26), to histone 3 lysine 27 acetylation (H3K27ac) that is correlated with open chromatin architecture (27). The data in Fig. 7A clearly shows that H3K27me3 modification is highly enriched in IRF-8 3rd intron in NIH3T3 cells in comparison to RAW cells while the opposite was observed for the H3K27ac modification; enriched in RAW cells. Together, these results support the FAIRE data and point to a dense chromatin architecture in IRF-8 restrictive cells.

To further establish these results, we also analyzed the abundance of these chromatin modifications in murine primary hematopoietic restricting cells such as Granulocyte\Macrophage Progenitors (GMPs) cells in comparison to permissive Bone-marrow Derived Macrophage (BMDM) cells. BM cells were harvested and grown

under conditions supporting the differentiation of these two cell types (detailed under Materials and Methods). Seven days later, ChIP analysis across IRF-8 3rd intron in these cell types was performed as detailed in Fig.7B. The two tested histone PTMs exhibited differential enrichment pattern between GMP (restrictive) and BMDM (permissive) cells. Histone PTM H3K27me₃, associated with condensed chromatin architecture, exhibited higher enrichment level in GMPs (Fig.7B). Conversely, histone PTM H3K27ac, associated with open chromatin architecture, exhibited higher enrichment levels in BMDM cells (Fig.7B). Similar results (data not shown) were also obtained with 32D.cl3 cell line that serves as model cell line for myeloid progenitor cells holding the potential to differentiate into either monocyte or granulocyte lineages (28). Like myeloid progenitor cells, this cell line does not express IRF-8 (data not shown). Taken together, this epigenetic “signature” exhibited in cell lines and *in-vivo* bone marrow derived cells, indicates that specific chromatin remodeling is a hallmark of myelopoiesis in general and differentiation of GMP cells to the monocyte\macrophage lineage in particular. Many more examples of this specific epigenetic signature over the IRF-8 3rd intron were published at the ENCODE database at a later stage since the onset of this research (elaborated under Discussion).

Inhibition of H3K27me₃ PTM leads to partial alleviation of IRF-8 suppression in restrictive cells

Polycomb-group (PcG) proteins elicit chromatin remodeling through epigenetic modifications that lead to gene silencing. PcGs reside in two multi-protein complexes: Polycomb Repressive Complex 1 and 2 (PRC1 and PRC2). Enhancer of zeste homolog 2 (EZH2), is the catalytic subunit of PRC2 silencing transcription through H3K27 trimethylation (29, 30). To test the possibility that inhibition of this modification will affect chromatin architecture resulting in alleviated IRF-8 expression we used

Adenosine dialdehyde (AdOx), an inhibitor of S-adenosylmethionine (AdoMet)-dependent methyltransferases (31). Addition of AdOx to NIH3T3 cells harboring BAC-IRF-8.1 reporter construct alleviated the restriction on endogenous IRF-8 as well as on the reporter gene expression (Fig 8). About 13% of the treated cells exhibited significant increase in the expression level of both the endogenous IRF-8 and the reporter gene, EGFP, as was evident by Fluorescence-Activated Cell Sorter (FACS) staining of individual cells (Fig. 8A). A significant shift in the expression peaks corresponding to the stained IRF8 and the fluorescence of EGFP in AdOx treated NIH3T3 was also evident (Fig. 8B). Together, these results indicate that the suppressive histone PTM, H3K27me3, is part of the regulatory mechanism leading to IRF-8 active repression in restrictive cells. The concurrent change in both the endogenous IRF-8 and its EGFP reporter gene underlies the authentic report of BAC-IRF-8.1 construct and the validity of BAC transgenesis as a reliable reporter system.

MafK is a mediator of IRF-8 repression in restrictive cells

Our results thus far point to an active repression mechanism of IRF-8 in restrictive cells mediated in part by its 3rd intron. Since deletion of the 3rd intron is sufficient to lift the lineage specific repression, we speculate that there are specific DBPs that bind the 3rd intron and recruit the epigenetic machinery. To identify such repressive mechanism we used a pooled barcoded Lentiviral shRNA Library (32) in search of putative repressor(s) using NIH3T3 cells harboring BAC-IRF-8.1 as a reporting cell line. We reasoned that knockdown of putative repressive protein(s) would lead to the alleviation of IRF-8 repression in this restrictive cell line that will be enriched by FACS through subsequent expression of the fluorescent reporter gene. For that purpose, we used Decipher pooled Lentiviral shRNA library module 1, targeting signaling pathways (including TFs and chromatin modifiers) (16). Each gene in this pooled library is targeted by 5-7 different

shRNA expression constructs, which are identifiable by barcode sequences. The target cell line NIH3T3 harboring BAC-IRF-8.1 was infected in three replicates with Lentiviral particles at a multiplicity of infection of 0.7. Positively infected cells were selected by addition of Puromycin for 72 hrs. Following selection, each replicate was subjected to FACS enrichment of the top 5% fluorescent cells and low 50% fluorescent cells as control (detailed under Materials and Methods). Genomic DNA was extracted from each cell population and following two rounds of PCR amplifications were subjected to next generation sequencing. The sequencing data was analyzed by specific statistical tools provided with the Decipher library (16). A positive hit was considered if two different shRNAs for the same gene led to significant augmentation (2 fold or higher) of the reporter gene. Interestingly, among the top 10 hits was MafK. MafK has putative binding site within a conserved segment (CNS3, Fig. 2) of IRF-8 3rd intron. EMSA analyses with a synthetic Double Stranded (DS) DNA probe corresponding to CNS3 harboring the MafK putative DNA binding site (Fig. 9), clearly indicate specific binding of the MafK binding site in restrictive NIH3T3. Corresponding unlabeled synthetic DS oligonucleotide with mutated MafK binding site did not compete for the binding in comparison to native unlabeled competitor DNA (Fig. 9A lanes 8-10 in comparison to lanes 5-7, respectively). Such specific binding was not observed in RAW cells as both specific and mutated unlabeled synthetic DS oligonucleotides competed equally for the binding (Fig. 9B lanes 8-10 in comparison to lanes 5-7, respectively). Western blot analysis demonstrated similar levels of MafK expression in both cell lines (data not shown). Interestingly, a strong *in-vivo* binding peak within the IRF-8 locus in general and the 3rd intron in particular was noted by ChIP analysis as evident by the ENCODE data base (33) (see supplemental Fig. S2). Furthermore, the reporter cell line, NIH3T3 cells harboring BAC-IRF-8.1, was transduced with lentiviral vector encoding

for shRNA directed against MafK in comparison to empty vector. The cells were taken for FACS analysis to monitor in each cell the reporter gene (EGFP) level as well as level of the endogenous IRF-8 (antibody staining). It is clear that significant alleviation of both the reporter gene and the endogenous IRF-8 within the same cell were observed in 56% of the cell population (Fig. 10). Taken together, these results point to the possible role of MafK as a chromatin effector protein of the IRF-8 locus in restrictive cells probably by interacting with IRF-8 3rd intron. Additionally, the fact that both the reporter gene and the endogenous IRF-8 gene expression were alleviated in the same cells is an additional strong support for the genuine authenticity of the BAC reporter system.

Discussion

IRF-8 is a member of the IRF family, which is expressed in a lineage restricted manner and play a key role in lineage commitment, cell type development, and functionality of mature macrophages, dendritic cells and B-cells (34-37). Mice with IRF-8 null mutation are defective in the ability of myeloid progenitor cells to mature toward macrophage lineage and eventually develop Chronic Myelogenous Leukemia (CML)-like syndrome. Taken together, IRF-8 acts both as an orchestrating factor of myeloid cell differentiation and as a myeloleukemia suppressor gene. This study was aimed at identifying the regulatory element responsible for IRF-8 restricted expression and gaining insight to the molecular mechanisms governing this restricted expression pattern.

The results with the various BAC IRF-8 reporter constructs clearly indicate that the 3rd intron of the IRF-8 gene acts as an intragenic regulatory element governing the expression of IRF-8 in restricting cells, i.e. non-immune cells. This points to a unique regulatory element in a non-coding intronic segment that has global effect on IRF-8 expression possibly by affecting the promoter and other intergenic regulatory elements. Intragenic elements affecting gene expression were described. For example, an intronic segment was identified as crucial for the B-cell restricted expression of Pax5 (18). The Pax5 lineage specific expression is dependent upon active enhancer element located within the 5th intron. This intronic enhancer serves as the binding site for B-cell specific transcription factors that lead to Pax5 expression and subsequent B-cell differentiation (18). However, while this is an intronic enhancer, the 3rd intron of IRF-8 mediates active repression in restrictive cells. Furthermore, deletion of each of the three CNSs within this intron revealed a gradual alleviation of repression of the IRF-8 reporter gene; the

strongest alleviation was noted with CNS2 deletion while the weakest with CNS1 (Fig. 5). The fact that deletion of each CNS separately resulted in alleviation indicates that each CNS is contributing to the active repression of IRF-8 in restrictive cells. Since repressed chromatin state is characteristic of the IRF-8 locus in general and the 3rd intron in particular in restricting cells, it suggests that interacting factors binding to each CNS may act in concert to elicit this chromatin-repressed state.

Our results point to the possible role of IRF-8 3rd intron as a nucleation core for chromatin condensation in restricting cells. Supporting this is the fact that only deletion of the IRF-8 3rd intron by the vCRE-VLoxP recombinase system prior to transfection led to the alleviation of IRF-8 reporter gene while removal of the intron within cells had no effect on the repressed state of the reporter gene. The latter suggests that the initial onset of a repressed chromatin is followed by the establishment of an "epigenetic memory". This "memory" is composed of define set of histone PTMs (38) that are spread along the IRF-8 locus in an undulation motion. Consequently, removal of the nucleation core, i.e. the 3rd intron, after the establishment of epigenetic memory has no longer effect on chromatin state. Taken together, the 3rd intron serves as cue site for the IRF-8 locus serving as a platform for cell-type specific DNA interacting factors during the differentiation process of cells. In non-hematopoietic cells, these factors initiate histone PTMs that lead to change in chromatin architecture followed by subsequent modifications that are the hallmark of the epigenetic memory. Supporting this is our observation that IRF-8 3rd intron is capable of repressing a luciferase reporter gene only when inserted to a retroviral vector that randomly integrates to the genome and assembles chromatin conformation in restrictive cells. This does not take place in permissive cells or if the 3rd intron is cloned in near the luciferase gene in expression

plasmid in transient transfection assays, where the transfected DNA does not assemble proper chromatin structure (39).

It is well established that histone PTM composition is directly linked to chromatin architecture (26, 40). Our results reveal higher nucleosome occupancy over the 3rd intron of IRF-8 in restrictive cell lines that is accompanied by H3K27me3 enrichment. Treatment of the restrictive cell line NIH3T3 with AdOx, an inhibitor of H3K27me3 PTM (Fig. 8), significantly alleviates this restrictive phenotype. H3K27me3 methylation is mediated by the PRC2 complex highlighting its role in mediating chromatin condensation and the subsequent silencing of IRF-8 in restrictive cells. This is supported by the genome-wide study by Bracken *et al.* annotating PcG targets, among which is the IRF-8 locus (41). This H3K27me3 mediated repression mechanism is functional in restrictive cells of non-hematopoietic origin as well as in myeloid progenitor cells of hematopoietic origin (GMP and 32D cells). Support for our results is also derived from the ENCODE project datasets (42) showing the same H3K27me3 enrichment pattern over the IRF-8 locus in restrictive cell lines such as normal human lung Fibroblast, as opposed to no enrichment in a permissive cell line, human Monocytes, (supplemental Fig.S3). The fact that AdOx alleviated both the endogenous IRF-8 as well as the IRF-8 BAC reporter gene expression underlies the authenticity of the BAC IRF-8 reporter system.

Finally, in an attempt to identify possible chromatin remodeling factors that affect IRF-8 expression, we have used a pooled barcoded shRNA lentiviral library. Among the top 10 hits was MafK. Expression of shRNA corresponding to MafK in our NIH3T3 IRF-8 reporter cell line not only alleviated the reporter gene but also alleviated the endogenous IRF-8 gene in the same cells (Fig. 10). Nearly 56% of the NIH3T3 cells harboring the BAC IRF-8 reporter exhibited alleviation of the two genes. Further,

EMSA analysis demonstrates that MafK binds to CNS3 (Fig. 9). Additionally, deletion of the whole CNS3 also led to partial alleviation of the reporter gene expression (Fig. 5). MafK is a crucial regulator of mammalian gene expression, a member of the Maf oncoproteins, and functions as both transcription activator and repressor by forming diverse heterodimers to bind DNA elements termed Maf recognition elements (43). Interestingly, the association between MafK and Methionine Adenosyltransferase (MAT) II α was reported (44). The latter is the source of S-adenosylmethionine which serves as a donor of methyl groups for Histone methylation such as; H3K4, H3K4 dimethylation and H3K27 trimethylation leading to repressed chromatin (45). Knockdown of MafK results in a significant decrease in MafK binding and therefore less recruitment of MATII α to target sites. Consequently, this major source for H3K27me₃ is inaccessible thus contributing to change in chromatin architecture e.g. alleviation of IRF-8 expression in restrictive cells. This is in agreement with our results using AdOx, a MATII α inhibitor, which also resulted in a significant rescue of both the expression of the endogenous IRF-8 as well as that of BAC IRF-8 reporter in NIH3T3 restrictive cells (Fig. 8). Additionally, association with HDAC proteins was also reported (43), which can add to the level of alleviation. Finally, *in-vivo* MafK binding along the IRF-8 coding region is observed by CHIP-seq analysis in IRF-8 restrictive CH12 B-cell lymphoma and not in embryonic stem cell line E14 harboring Naïve chromatin (ENCODE database, supplemental Fig. 2S).

Our results strongly suggest that H3K27me₃ histone PTM, which leads to dense chromatin architecture, is a key element in IRF-8 lineage specific repression. Therefore, we propose that IRF-8 3rd intron serves as a "nucleation core" for H3K27 trimethylation for the entire IRF-8 locus. One possible scenario is that MafK cooperates with other factors (to be identified) to recruit chromatin modifiers (like MATII α (45))

via protein-protein interactions. These complexes might serve as molecular cues for the PRC2 complex, which is responsible for the tri-methylation of H3K27. Additionally, as shown by Yuan *et al.* (46), the 3rd intron dense chromatin structure itself may serve as a Polycomb Response Element (PRE) recruiting PRC2 complex. This will lead eventually to the modification of flanking nucleosomes in a wave motion directing the spread of H3K27 tri-methylation across the entire IRF-8 locus (46). This mechanism does not exclude the possibility that the IRF-8 3rd intron is also engaged in intra-locus looping with the promoter region thus eliciting direct repression in restrictive cells. The IRF-8 3rd intron might serve as an "anchorage point" for various *trans*-acting regulatory machineries such as PRC1/2 complexes. PRC1 binding through the PcG chromodomain (CHD) utilizes intra-locus looping to interact with other PcG Response Element (PRE) in the promoter region, such as CpG islands. These interactions stabilize intragenic looping and facilitate the spread of the repressive histone mark throughout the IRF-8 locus (47). It is yet to be determined whether MafK is among the recruiting factors of the PRC1/2 complexes in IRF-8 restricting cells.

Acknowledgement

We acknowledge the contribution of past members of the Levi's laboratory, Mr. Ron Shalom and Mrs. Revital Schick for their valuable contributions at the early stages of this project. This research was funded by The Israel Science Foundation (121/10) to B.Z.L. B.Z.L. is an incumbent of the Lily and Silvian Marcus Chair in Life Sciences, Technion.

References

1. Doulatov S, Notta F, Laurenti E, Dick John E. Hematopoiesis: A Human Perspective. *Cell Stem Cell*. 2012;10(2):120-36. doi: <http://dx.doi.org/10.1016/j.stem.2012.01.006>.
2. Rosmarin AG, Yang Z, Resendes KK. Transcriptional regulation in myelopoiesis: Hematopoietic fate choice, myeloid differentiation, and leukemogenesis. *Experimental hematology*. 2005;33(2):131-43.
3. Geissmann F, Manz MG, Jung S, Sieweke MH, Merad M, Ley K. Development of monocytes, macrophages, and dendritic cells. *Science*. 2010;327(5966):656-61.
4. Rosenbauer F, Tenen DG. Transcription factors in myeloid development: balancing differentiation with transformation. *NatRevImmunol*. 2007;7(2):105-17.
5. Gordon S. Alternative activation of macrophages. *Nature Reviews Immunology*. 2003;3(1):23-35.
6. Giraldo P, Montoliu L. Size matters: use of YACs, BACs and PACs in transgenic animals. *Transgenic Res*. 2001;10(2):83-103.
7. Takaoka A, Yanai H. Interferon signalling network in innate defence. *Cell Microbiol*. 2006;8(6):907-22.
8. Burchert A, Cai D, Hofbauer LC, Samuelsson MKR, Slater EP, Duyster J, et al. Interferon consensus sequence binding protein (ICSBP; IRF-8) antagonizes BCR/ABL and down-regulates bcl-2. *Blood*. 2004;103(9):3480-9.
9. Sparwasser T, Eberl G. BAC to immunology--bacterial artificial chromosome-mediated transgenesis for targeting of immune cells. *Immunology*. 2007;121(3):308-13.
10. Muyrers JPP, Zhang Y, Testa G, Stewart AF. Rapid modification of bacterial artificial chromosomes by ET-recombination. *Nucleic Acids Res*. 1999;27(6):1555-7.
11. Suzuki E, Nakayama M. VCre/VloxP and SCre/SloxP: new site-specific recombination systems for genome engineering. *Nucleic Acids Res*. 2011;39(8):e49. Epub 2011/02/04. doi: 10.1093/nar/gkq1280. PubMed PMID: 21288882; PubMed Central PMCID: PMC3082901.
12. Simon JM, Giresi PG, Davis IJ, Lieb JD. Using formaldehyde-assisted isolation of regulatory elements (FAIRE) to isolate active regulatory DNA. *Nature Protocols*. 2012;7(2):256-67.
13. Nelson JD, Denisenko O, Bomsztyk K. Protocol for the fast chromatin immunoprecipitation (ChIP) method. *Nature Protocols*. 2006;1(1):179-85.
14. Pattyn F, Speleman F, De Paepe A, Vandesompele J. RTPrimerDB: the real-time PCR primer and probe database. *Nucleic Acids Res*. 2003;31(1):122-3. Epub 2003/01/10. PubMed PMID: 12519963; PubMed Central PMCID: PMC3082901.
15. Makinde TO, Agrawal DK. Increased expression of angiopoietins and Tie2 in the lungs of chronic asthmatic mice. *American journal of respiratory cell and molecular biology*. 2011;44(3):384-93. Epub 2010/05/14. doi: 10.1165/rcmb.2009-0330OC. PubMed PMID: 20463289; PubMed Central PMCID: PMC3095938.

16. Collecta I. The DECIPHER open source RNAi Screening Project: Collecta, Inc.; 2013 [cited 2013 July]. Available from: <http://www.decipherproject.net/shRNA-libraries/>.
17. Alter-Koltunoff M, Ehrlich S, Dror N, Azriel A, Eilers M, Hauser H, et al. Nramp1 mediated innate resistance to intraphagosomal pathogens is regulated by IRF-8, PU.1 and Miz-1. *J Biol Chem*. 2003;278(45):44025-32.
18. Decker T, Pasca dM, McManus S, Sun Q, Bonifer C, Tagoh H, et al. Stepwise activation of enhancer and promoter regions of the B cell commitment gene Pax5 in early lymphopoiesis. *Immunity*. 2009;30(4):508-20.
19. Chandler KJ, Chandler RL, Broeckelmann EM, Hou Y, Southard-Smith EM, Mortlock DP. Relevance of BAC transgene copy number in mice: transgene copy number variation across multiple transgenic lines and correlations with transgene integrity and expression. *Mamm Genome*. 2007;18(10):693-708.
20. Schonheit J, Kuhl C, Gebhardt ML, Klett FF, Riemke P, Scheller M, et al. PU.1 level-directed chromatin structure remodeling at the *Irf8* gene drives dendritic cell commitment. *Cell reports*. 2013;3(5):1617-28. doi: 10.1016/j.celrep.2013.04.007. PubMed PMID: 23623495.
21. Simon JA, Kingston RE. Occupying chromatin: Polycomb mechanisms for getting to genomic targets, stopping transcriptional traffic, and staying put. *Mol Cell*. 2013;49(5):808-24. Epub 2013/03/12. doi: 10.1016/j.molcel.2013.02.013. PubMed PMID: 23473600; PubMed Central PMCID: PMC3628831.
22. Ovcharenko I, Nobrega MA, Loots GG, Stubbs L. ECR Browser: a tool for visualizing and accessing data from comparisons of multiple vertebrate genomes. *Nucleic Acids Res*. 2004;32(Web Server issue):W280-6. Epub 2004/06/25. doi: 10.1093/nar/gkh355. PubMed PMID: 15215395; PubMed Central PMCID: PMC441493.
23. Genomatix. Genomatix Software Suite [cited 2012 September 1st]. Available from: <http://www.genomatix.de/solutions/genomatix-software-suite.html>.
24. Martinez-Garcia E, Licht JD. Dereglulation of H3K27 methylation in cancer. *Nat Genet*. 2010;42(2):100.
25. Bernstein BE, Meissner A, Lander ES. The mammalian epigenome. *Cell*. 2007;128(4):669-81. Epub 2007/02/27. doi: 10.1016/j.cell.2007.01.033. PubMed PMID: 17320505.
26. Kouzarides T. Chromatin modifications and their function. *Cell*. 2007;128(4):693-705. Epub 2007/02/27. doi: 10.1016/j.cell.2007.02.005. PubMed PMID: 17320507.
27. Creighton MP, Cheng AW, Welstead GG, Kooistra T, Carey BW, Steine EJ, et al. Histone H3K27ac separates active from poised enhancers and predicts developmental state. *Proceedings of the National Academy of Sciences*. 2010;107(50):21931-6.
28. Valtieri M, Tweardy D, Caracciolo D, Johnson K, Mavilio F, Altmann S, et al. Cytokine-dependent granulocytic differentiation. Regulation of proliferative and differentiative responses in a murine progenitor cell line. *The Journal of Immunology*. 1987;138(11):3829-35.
29. Li KK, Luo C, Wang D, Jiang H, Zheng YG. Chemical and biochemical approaches in the study of histone methylation and demethylation. *Medicinal research reviews*. 2012;32(4):815-67.

30. Johnson BA, Najbauer J, Aswad DW. Accumulation of substrates for protein L-isoaspartyl methyltransferase in adenosine dialdehyde-treated PC12 cells. *J Biol Chem.* 1993;268(9):6174-81.
31. Bartel RL, Borchardt RT. Effects of adenosine dialdehyde on S-adenosylhomocysteine hydrolase and S-adenosylmethionine-dependent transmethylation in mouse L929 cells. *Mol Pharmacol.* 1984;25(3):418-24. Epub 1984/05/01. PubMed PMID: 6727864.
32. Mohr Stephanie CBaNP. Genomic screening with RNAi: results and challenges. *Annu Rev Biochem.* 2010;79:37-64.
33. Rosenbloom KR, Sloan CA, Malladi VS, Dreszer TR, Learned K, Kirkup VM, et al. ENCODE Data in the UCSC Genome Browser: year 5 update. *Nucleic Acids Res.* 2013;41(D1):D56-D63.
34. Dror N, Alter-Koltunoff M, Azriel A, Amariglio N, Jacob-Hirsch J, Zeligson S, et al. Identification of IRF-8 and IRF-1 target genes in activated macrophages. *Mol Immunol.* 2007;44(4):338-46. Epub 2006/04/07. doi: S0161-5890(06)00082-4 [pii] 10.1016/j.molimm.2006.02.026. PubMed PMID: 16597464.
35. Tamura T, Yanai H, Savitsky D, Taniguchi T. The IRF family transcription factors in immunity and oncogenesis. *AnnuRevImmunol.* 2008;26:535-84.
36. Tamura T, Thotakura P, Tanaka TS, Ko MS, Ozato K. Identification of target genes and a unique cis element regulated by IRF-8 in developing macrophages. *Blood.* 2005;106(6):1938-47.
37. Wang H, Morse HC, III. IRF8 regulates myeloid and B lymphoid lineage diversification. *ImmunolRes.* 2009;43(1-3):109-17.
38. Campos EI, Stafford JM, Reinberg D. Epigenetic inheritance: histone bookmarks across generations. *Trends Cell Biol.* 2014. Epub 2014/09/23. doi: 10.1016/j.tcb.2014.08.004. PubMed PMID: 25242115.
39. Jeong S, Stein A. Micrococcal nuclease digestion of nuclei reveals extended nucleosome ladders having anomalous DNA lengths for chromatin assembled on non-replicating plasmids in transfected cells. *Nucleic Acids Res.* 1994;22(3):370-5. Epub 1994/02/11. PubMed PMID: 7510391; PubMed Central PMCID: PMC523591.
40. Lee JS, Smith E, Shilatifard A. The language of histone crosstalk. *Cell.* 2010;142(5):682-5. Epub 2010/09/04. doi: 10.1016/j.cell.2010.08.011. PubMed PMID: 20813257.
41. Bracken AP, Dietrich N, Pasini D, Hansen KH, Helin K. Genome-wide mapping of Polycomb target genes unravels their roles in cell fate transitions. *Genes & development.* 2006;20(9):1123-36.
42. Bernstein B, Birney E, Dunham I, Green E, Gunter C, Snyder M. An integrated encyclopedia of DNA elements in the human genome. *Nature.* 2012;489(7414):57.
43. Kannan MB, Solovieva V, Blank V. The small MAF transcription factors MAFF, MAFG and MAFK: current knowledge and perspectives. *Biochim Biophys Acta.* 2012;1823(10):1841-6. Epub 2012/06/23. doi: 10.1016/j.bbamcr.2012.06.012. PubMed PMID: 22721719.

44. Katoh Y, Ikura T, Hoshikawa Y, Tashiro S, Ito T, Ohta M, et al. Methionine adenosyltransferase II serves as a transcriptional corepressor of Maf oncoprotein. *Mol Cell*. 2011;41(5):554-66. Epub 2011/03/03. doi: 10.1016/j.molcel.2011.02.018. PubMed PMID: 21362551.
45. Igarashi K, Katoh Y. Metabolic aspects of epigenome: coupling of S-adenosylmethionine synthesis and gene regulation on chromatin by SAMIT module. *Sub-cellular biochemistry*. 2013;61:105-18. Epub 2012/11/15. doi: 10.1007/978-94-007-4525-4_5. PubMed PMID: 23150248.
46. Yuan W, Wu T, Fu H, Dai C, Wu H, Liu N, et al. Dense Chromatin Activates Polycomb Repressive Complex 2 to Regulate H3 Lysine 27 Methylation. *Science*. 2012;337(6097):971-5.
47. Grewal SI, Moazed D. Heterochromatin and epigenetic control of gene expression. *Science*. 2003;301(5634):798-802. Epub 2003/08/09. doi: 10.1126/science.1086887. PubMed PMID: 12907790.
48. Akashi K, Traver D, Miyamoto T, Weissman IL. A clonogenic common myeloid progenitor that gives rise to all myeloid lineages. *Nature*. 2000;404(6774):193-7. Epub 2000/03/21. doi: 10.1038/35004599. PubMed PMID: 10724173.
49. Arai F, Hirao A, Ohmura M, Sato H, Matsuoka S, Takubo K, et al. Tie2/angiopoietin-1 signaling regulates hematopoietic stem cell quiescence in the bone marrow niche. *Cell*. 2004;118(2):149-61. Epub 2004/07/21. doi: 10.1016/j.cell.2004.07.004
S0092867404006622 [pii]. PubMed PMID: 15260986.
50. Gordon S, Taylor PR. Monocyte and macrophage heterogeneity. *Nat Rev Immunol*. 2005;5(12):953-64. Epub 2005/12/03. doi: nri1733 [pii]
10.1038/nri1733. PubMed PMID: 16322748.
51. Kent WJ, Sugnet CW, Furey TS, Roskin KM, Pringle TH, Zahler AM, et al. The human genome browser at UCSC. *Genome Res*. 2002;12(6):996-1006. Epub 2002/06/05. doi: 10.1101/gr.229102. Article published online before print in May 2002. PubMed PMID: 12045153; PubMed Central PMCID: PMC186604.

Figure Legends

Fig. 1 - Deletion analysis using BAC-IRF-8 reporter constructs points to the role of the 3rd intron in modulating lineage specific expression of IRF-8

The murine BAC genomic clone 7H10 was used for generating BAC reporter constructs for the IRF-8 locus by the Red ET cloning system. Schematic illustrations of the various BAC-IRF-8 constructs, to which a cassette containing a fluorescent reporter (mCherry) and a selectable marker (Neo driven by the PKG promoter) was inserted, are shown. A) BAC IRF-8.1- the cassette was inserted to the first ATG. B) BAC IRF-8.2- the cassette was swapped with the entire IRF-8 coding region (CDS). C) The reporter construct BAC IRF-8.3 is similar to that illustrated in panel A except that the 2nd intron was deleted. D) The reporter construct BAC IRF-8.4 is similar to that illustrated in panel A except that the 3rd intron was deleted. Exons (black boxes) are numbered. RAW and NIH3T3 cells were transfected with the various BAC constructs and at least 10 stable clones were isolated. The copy number of the inserted clone was determined by qPCR. The fluorescence activity of the reporter gene in representative RAW and NIH3T3 stable clones harboring 1-2 copies of the BAC reporter construct was visualized under fluorescent microscope before and following 16 hrs of exposure to IFN- γ (100U/ml) as indicated in the i section of each panel in the Figure. Additionally, RNA was extracted from each clone before and following treatment with IFN- γ and the Fold of Induction levels of the reporter gene and the endogenous IRF-8 were determined by real-time qRT-PCR and shown in the ii section of each panel in the figure.

Fig. 2 - Bioinformatics analysis of IRF-8 coding region with special detail on the 3rd intron

The upper panel illustrates comparative sequence analysis of IRF-8 coding region using ECR Browser (22). Conserved sequences (sequences that are longer than 100bp and have a percent identity of at least of 70%) in the IRF-8 coding region between mouse, cow and human genomes are aligned. Exons are indicated in blue and conserved non-coding sequences (CNS) within the introns indicated in pink. The 2nd and the 3rd intron are boxed by dotted green lines. The lower panel illustrates zooming into the 3rd intron (1730bp) revealing three conserved regions between mouse (mm10 dataset) and human (hg19 dataset), designated Conserved Non-coding Sequences (CNS) 1, 2 and 3, boxed in red, blue, and green, respectively. MatInspector (Genomatix software suite (23)) analysis of putative TF binding motifs in IRF-8 3rd intron conserved regions revealed five dense clusters of putative binding sequences designated CNS1.1, CNS1.2 (located in CNS1), CNS2.1 (located in CNS2), CNS3.1 and CNS3.2 (located in CNS3).

Fig. 3- Only deletion of IRF-8 3rd intron prior to transfection to restrictive cells alleviated the reporter repression

A) NIH3T3 were transfected with BAC IRF-8.1 VLoxP. To induce 3rd intron deletion within the cells, stable clones were transduced with retroviral vector encoding for the VCre gene. After selection with Puromycin, clones were induced with IFN- γ (100 μ g/ml) for 16 hrs. Reporter (GFP) expression was monitored using cell observer microscopy. A representative clone harboring 1-2 BAC copies is shown in this panel.

B) The 3rd intron in BAC IRF-8.1 VLoxP construct was initially deleted with the corresponding VCre recombinase in *E. coli*. Subsequently the corresponding BAC DNA was transfected to NIH3T3 and stable clones were selected. Each clone was also induced with IFN- γ (100 μ g/ml) for 16 hrs and GFP expression was observed under microscopy. A representative clone harboring 1-2 BAC copies is shown in this panel.

Fig. 4 - IRF-8 3rd intron represses the expression of genomically integrated Luciferase only in restrictive cells

NIH3T3 and RAW cells (panels A and B, respectively) were transduced with either pMSCV-luciferase reporter construct (pMSCV-Luc) or with similar constructs harboring either IRF-8 3rd intron or GAPDH 2nd intron upstream to the reporter gene (pMSCV-Luc-int3 and pMSCV-Luc-GAPDHint2, respectively). 72 hrs later, cells were harvested and luciferase levels were measured. Relative luciferase expression was calculated. Data is given as mean of at least three different experiments. NIH3T3 show significant difference in luciferase level between cells transfected with pMSCV-Luc and pMSCV-Luc-int3 (Student's T test, $\alpha < 0.001$) whereas no significant difference is observed in Raw cells between the two constructs (Student's T test, $\alpha < 0.05$).

Fig. 5 - Fine deletions of the CNSs within IRF-8 3rd intron

BAC IRF-8.1 constructs harboring deletions in conserved regions were transfected to repressive NIH3T3 cells as described under Fig. 1 and stable clones were isolated. Representative isolated clones were plated and not treated or treated with IFN- γ (100 μ g/ml) for 16 hrs and EGFP fluorescence was observed under microscopy. Deletion of CNS1 (position 1-284, upper panel), deletion of CNS2 (position (680-860, middle panel) and deletion of CNS3 (Position1230-1730, lower panel).

Fig. 6 – Differential nucleosome occupancy across the IRF-8 3rd intron between RAW and NIH3T3 cells

RAW and NIH3T3 cell lines were subjected to FAIRE analysis for the enrichment of nucleosome depleted DNA. The 19 PCR amplicons spanning the entire 3rd intron are numbered. Nucleosome depleted DNA Fold of Enrichment was calculated for each cell line and presented as Fold Difference ratio between RAW and NIH3T3 cells as detailed under Materials and Methods. Results are the average of 3 independent FAIRE experiments (Mann Whitney U test, $\alpha=0.05$).

Fig. 7 – Differential histone PTM profile across the IRF-8 3rd intron between expression permissive and restrictive cells

RAW, NIH3T3 as well as bone marrow derived GMP and BMDM cells were subjected to ChIP using histone modification monoclonal antibodies directed against 3 histone PTMs; H3K27ac (black bars) and H3K27me3 (gray bars). The 19 PCR amplicons spanning the entire 3rd intron are numbered. Graphs represent the Fold Difference ratio between RAW and NIH3T3 cells (panel A) or between BMDM to GMP cells (panel B) as detailed under Materials and Methods. Results are the average of 3 independent ChIP experiments (Mann Whitney U test, $\alpha=0.05$).

Fig. 8 AdOx treatment alleviated both IRF-8 reporter gene and the endogenous IRF-8 in NIH3T3 restricting cells

NIH3T3 cells harboring BAC IRF8.1-EGFP construct were either untreated or treated with 25 μ M of AdOx. EGFP and IRF-8 expression were measured using flow cytometry. Representative dot plots (A) and overlay histograms (B) are shown. Dot plots quadrants were determined according to NIH3T3 WT cells stained with control IgG. Percentage of population co-expressing EGFP and IRF8 is indicated.

Fig. 9 – Binding to MafK binding site within CNS3 is detected by EMSA only with nuclear extract of restrictive cells

Specific binding to MafK binding site within CNS3 was observed by EMSA performed with nuclear extract (NE) from NIH3T3 and RAW (as indicated in the figure). Oligonucleotides corresponding to CNS3 were annealed and radio labeled. Nuclear extract of the two cell lines was reacted with the CNS3 probe in the absence or the presence of either unlabeled non-specific competitor (NS), specific competitor (S) or mutated competitor (mut) at 5, 10 and 20-fold molar excess over the labeled probe, as indicated in the figure. For details, see Materials and Methods.

Fig. 10 – MafK inhibition leads to the alleviation of both IRF-8 reporter gene and the endogenous IRF-8 in NIH3T3 restricting cells

NIH3T3 cells harboring BAC IRF8.1-EGFP construct were transfected with empty pLKO.1 lentiviral vector or the same vector harboring shRNA targeting MafK. Following antibiotic selection, EGFP and IRF-8 expression were measured using flow cytometry (detailed under Materials and Methods). Dot blot quadrants were determined according to unstained NIH3T3 WT cells. Percentage of population co-expressing EGFP and IRF8 is indicated.

Supporting Information

S1 Table. Primer pairs used in this study

The primers used for real-time PCR were designed using PrimerExpress software (ABI) or previously described. For each primer the target organism is designated.

Name		Sequence (5' → 3')	Organism
IRF-8 (cDNA)	For	GGCAGTGGCTGATCGAACA	Mouse
	Rev	GGTCTTCTCATCATTTTCCCAGA	Mouse
GAPDH (cDNA)	For	AGGTCGGTGTGAACGGATTTG	Mouse
	Rev	TGTAGACCATGTAGTTGAGGTCA	Mouse
IRF-1 (cDNA)	For	CAGAGGAAAGAGAGAAAGTCC	Mouse
	Rev	CACACGGTGACAGTGCTGG	Mouse
ChIP control (GAPDH) for αH3K4me3	For	TACTAGCGGTTTTACGGGCG	Mouse
	Rev	TCGAACAGGAGGAGCAGAGAGCGA	Mouse
ChIP control (GAPDH) for αH3K4me2	For	GGCTCCACCTTTCTCATCC	Mouse
	Rev	GGCCATCCACAGTCTTCTGG	Mouse
ChIP control (Human Alpha-satellite) For αH3K27me3	For	CTGCACTACCTGAAGAGGAC	Human
	Rev	GATGGTTCAACACTCTTACA	Human
ChIP control (human p21 promoter) for αH3K9ac	For	GTGGCTCTGATTGGCTTTCTG	Human
	Rev	CTGAAAACAGGCAGCCCAAG	Human

IRF-8 int3 amplicon1	For	AGGTTACGCTGTGCTCTGAACA	Mouse
	Rev	TCTAGCCCTGTGGAGACTGAGG	Mouse
IRF-8 int3 amplicon2	For	CCTCAGTCTCCACAGGGCTAGA	Mouse
	Rev	AAGAGAGAACAACCTCTGGTGAGCTAA	Mouse
IRF-8 int3 amplicon3	For	TTAGCTCACCAGAGTTGTTCTCTCTT	Mouse
	Rev	AGTTTATGCTGAGCTCCGGG	Mouse
IRF-8 int3 amplicon4	For	CCCGGAGCTCAGCATAAACT	Mouse
	Rev	AGGGAATCCTGCATCACAGACT	Mouse
IRF-8 int3 amplicon5	For	AGTCTGTGATGCAGGATTCCT	Mouse
	Rev	CACACCGAAGCCATCAGTGA	Mouse
IRF-8 int3 amplicon6	For	TGTGTCACTGCTGGAGAGGATAAC	Mouse
	Rev	GCCAGTGTGCGTTCATTCC	Mouse
IRF-8 int3 amplicon7	For	ATGAACGCACACTGGCCTTC	Mouse
	Rev	AGACAAAGGAGCCGGCCTT	Mouse
IRF-8 int3 amplicon8	For	CTCCTTTGTCTTCGCAGTGATTT	Mouse
	Rev	AGTCAGGGTCATTAACCAGATCAAG	Mouse
IRF-8 int3 amplicon9	For	CTTGATCTGGTTAATGACCCTGACT	Mouse
	Rev	AGAGAGGCAGGCAAACCACTC	Mouse
IRF-8 int3 amplicon11	For	GTCTCTCCACCTGGATGAAGC	Mouse
	Rev	CCCTGGGTACATTTGCCTCAGGA	Mouse

IRF-8 int3 amplicon12	For	GTTATTGTTCTGCTGTGTCTCATG	Mouse
	Rev	TGCTGACCCACTTTGTACCTCTT	Mouse
IRF-8 int3 amplicon13	For	AAGAGGTACAAAGTGGGTCAGCA	Mouse
	Rev	TGTATACGTGCCACATGGGG	Mouse
IRF-8 int3 amplicon14	For	CCCCATGTGGCACGTATACACA	Mouse
	Rev	AAGGTAGGGAGTGCCAGGTAA	Mouse
IRF-8 int3 amplicon15	For	ATGCACACGTATAAAAGGGCAA	Mouse
	Rev	GACAAGCGCCAGACTTTGG	Mouse
IRF-8 int3 amplicon16	For	CCAAAGTCTGGCGCTTGTC	Mouse
	Rev	TCTCATGGCCGGGTCATCT	Mouse
IRF-8 int3 amplicon17	For	AGATGACCCGGCCATGAGA	Mouse
	Rev	GGAGTAGTGAGCGTCCTTCGC	Mouse
IRF-8 int3 amplicon18	For	AGCAGCTGCTGGTCAAA	Mouse
	Rev	AGGGCAGCCGAGCACACTGC	Mouse
IRF-8 int3 amplicon19	For	CAGTGTGCTCGGCTGCC	Mouse
	Rev	TCCATCTCAGGAACTTCGCTC	Mouse
c-fms [M-CSF receptor]	For	AGCACGAGAACATCGTCAACC	Mouse
	Rev	TTCGCAGAAAGTTGAGCAGGT	Mouse
EZH2	For	AGCACAAGTCATCCCGTTAAAG	Mouse
	Rev	AATTCTGTTGTAAGGGCGACC	Mouse

Tie2	For	GATTTTGGATTGTCCCGAGGTCAAG	Mouse
	Rev	CACCAATATCTGGGCAAATGATGG	Mouse
CD34	For	AAGGCTGGGTGAAGACCCTTA	Mouse
	Rev	TGAATGGCCGTTTCTGGAAGT	Mouse

S1 Fig. Characterization of primary mouse bone marrow derived GMP and BMDM cells.

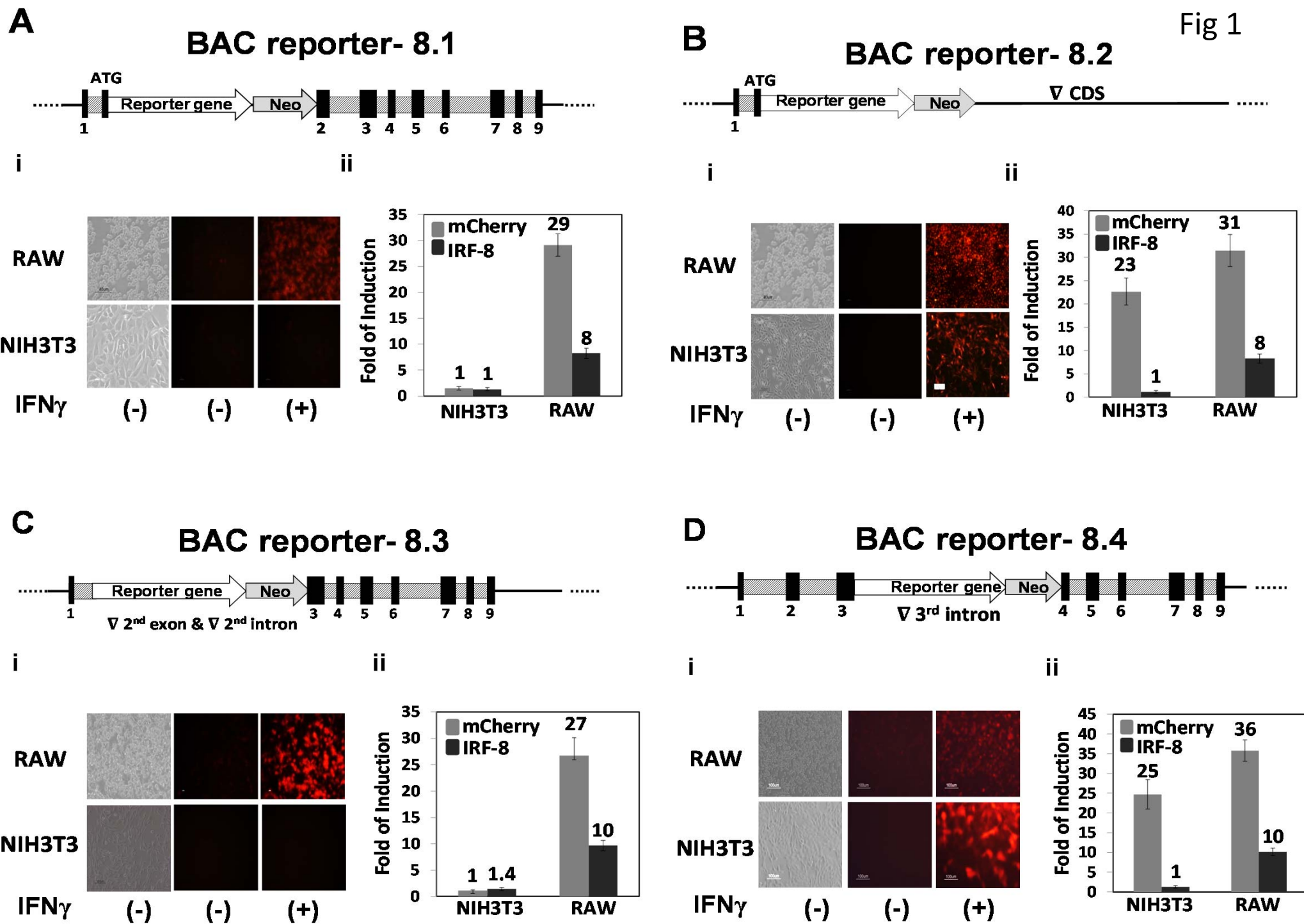
BM cells were harvested from the tibia and femur of 6-8 weeks old C57BL/6 mice, and cultivated with medium supplemented with IL-3 or M-CSF, resulting in GMP (CD34^{high}) and BMDM cells, respectively. Cell characteristics were determined by analyzing GMP associated gene markers, CD34 and Tie2 (48, 49) and macrophages associated marker, M-CSF receptor (50). A) Flow cytometry analysis of cell surface marker CD34 on GMP cells. Real-Time qPCR was employed to determine relative gene expression levels of CD34 (B), Tie2 (C) and M-CSF receptor (D). Expression level in BMDM cells was determined as 1. E) IRF-8 induced expression in GMP and BMDM cells. Cells were treated with IFN- γ for 16 hrs. IRF-8 expression level in untreated cells was determined as 1. Results shown are average \pm SEM of 3 independent experiments.

S2 Fig. MafK binding enrichment over the IRF-8 locus

In-vivo MafK binding over the IRF-8 coding region with emphasis on the 3rd intron (marked by red square) was aligned between murine CH12, B-cell lymphoma, (light blue), and embryonic stem cell cell line ES-E14 (dark blue). All experimental data are part of the ENCODE data set and were plotted with the UCSC genome browser (<http://encodeproject.org/ENCODE/>) (33, 51) that was made publically available by the BROAD institute.

S3 Fig. H3K27me3 binding enrichment over the IRF-8 locus

Comparison of H3K27me3 occupancy over the IRF-8 3rd intron (marked by red square) between two human cell types; Monocytes CD14+, IRF-8 permissive, and normal human lung fibroblasts (NHLF), IRF-8 restrictive. All experimental data are part of the ENCODE data set and were plotted with the UCSC genome browser (<http://encodeproject.org/ENCODE/>) (33, 51) that was made publically available by the BROAD institute.



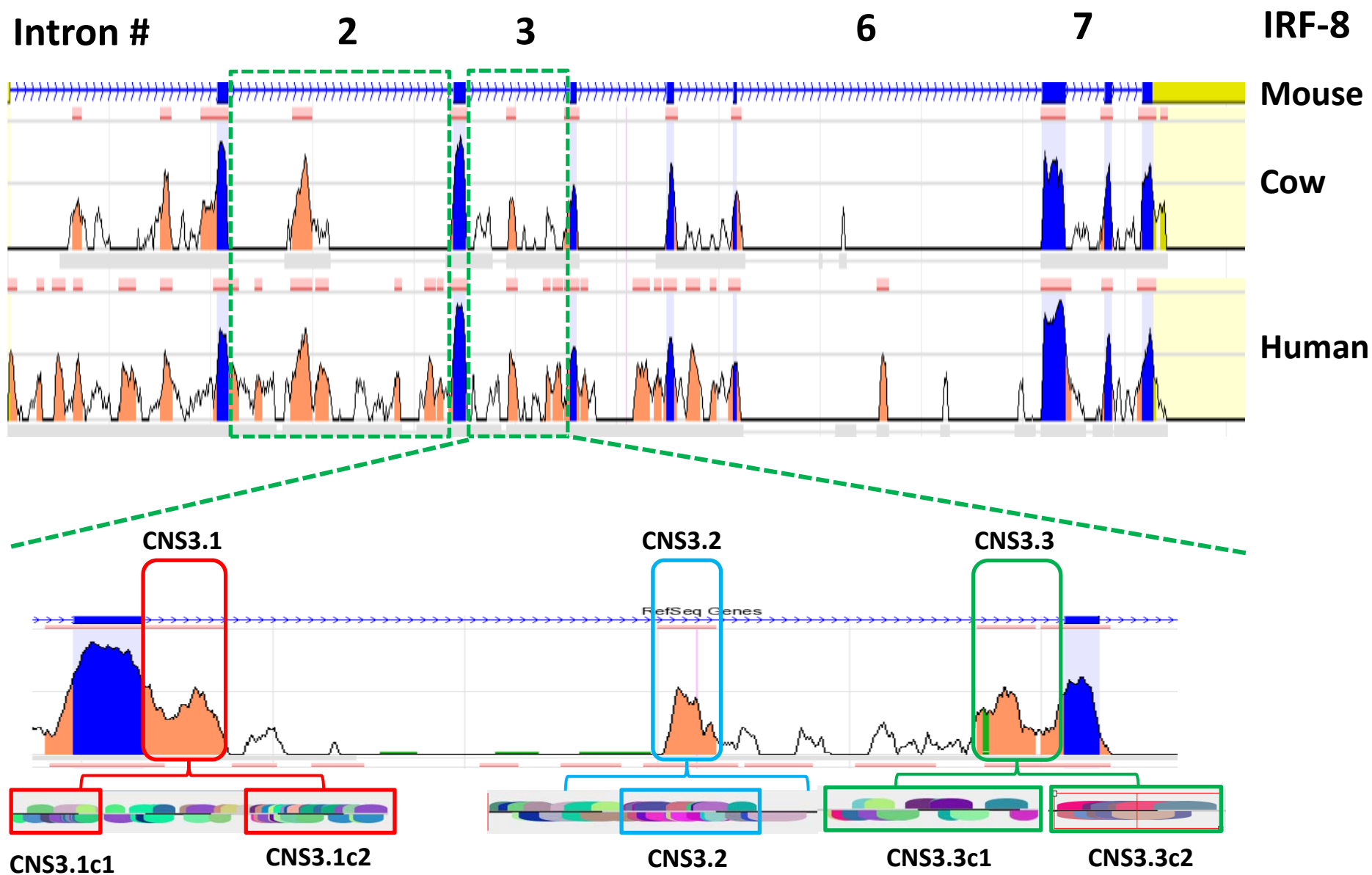


Fig 2

Fig 3

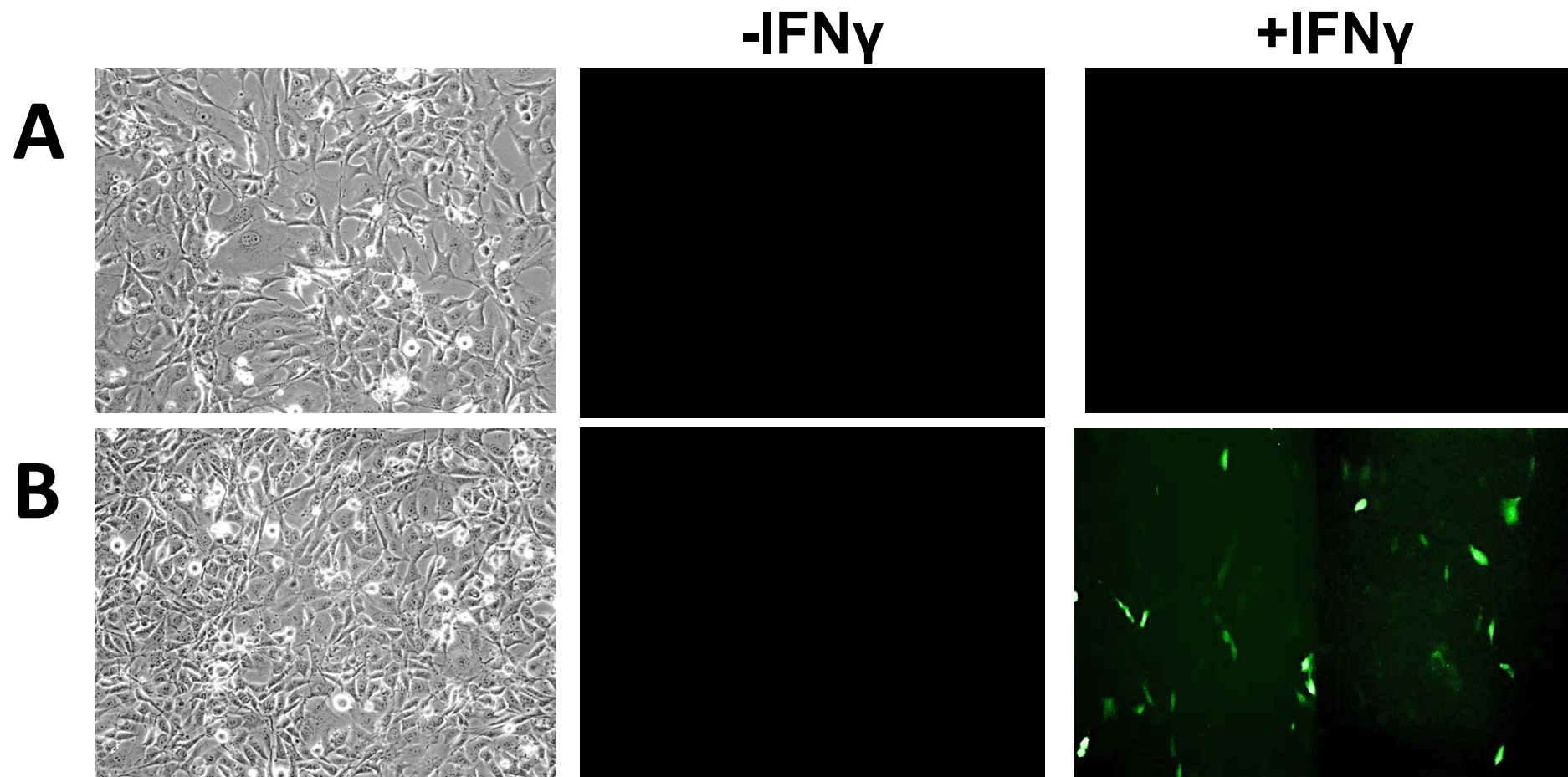


Fig 4

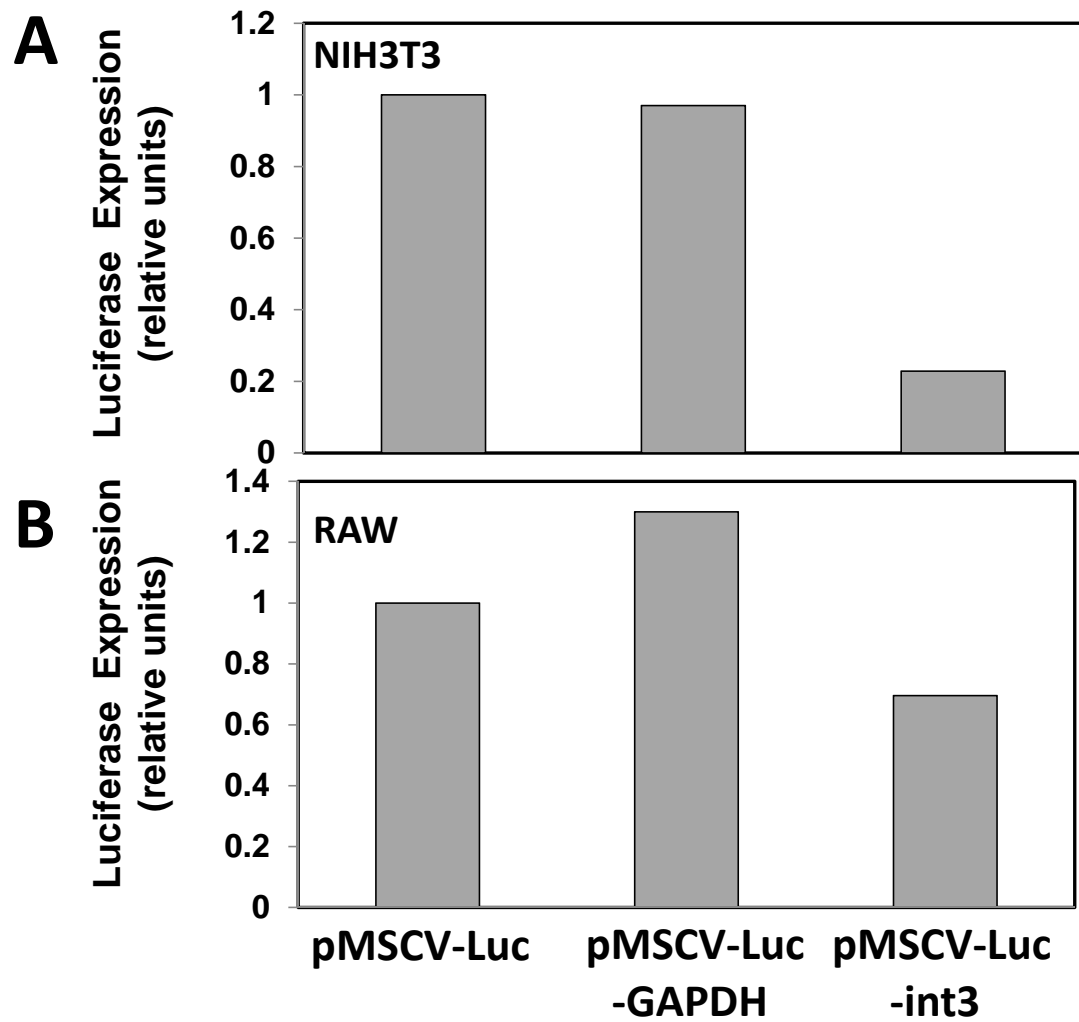
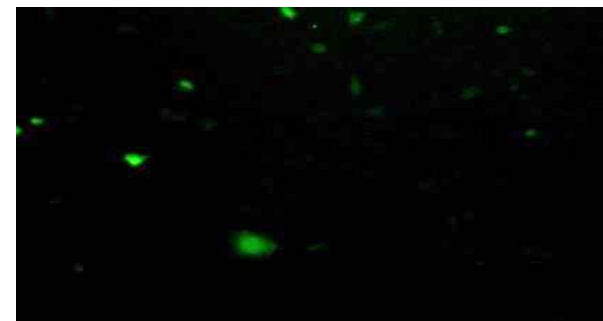
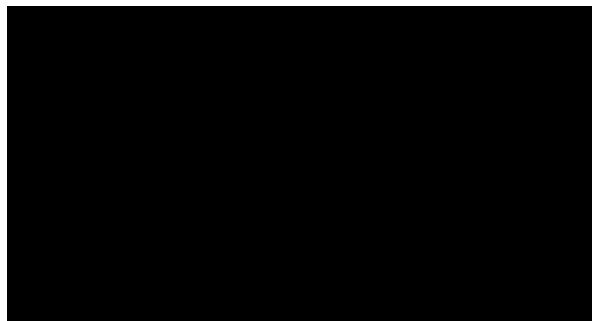
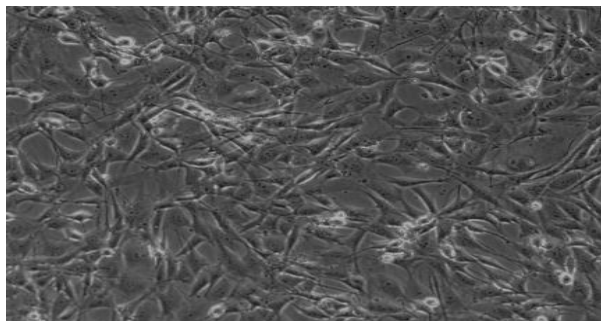


Fig 5

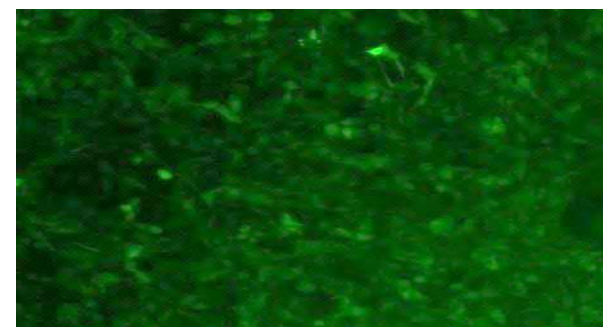
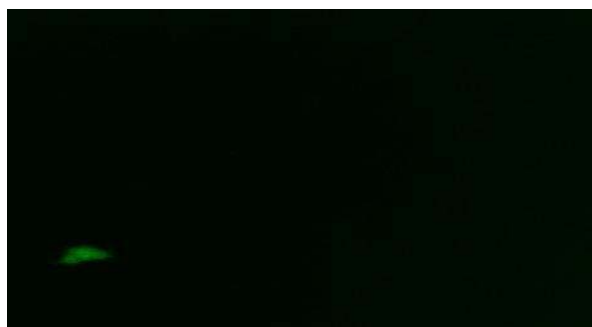
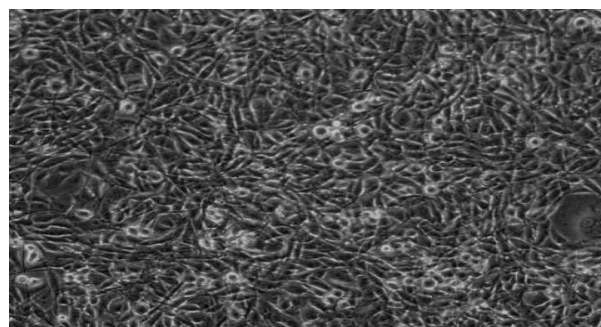
-IFN- γ

+IFN- γ

∇ CNS1



∇ CNS2



∇ CNS3

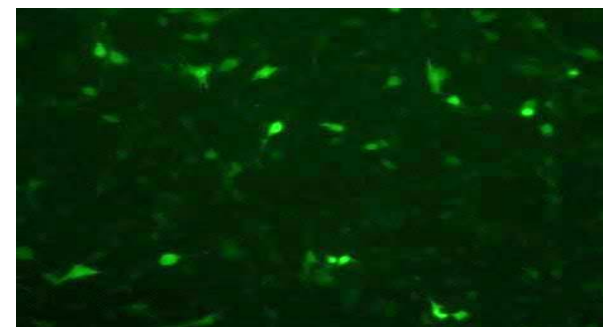
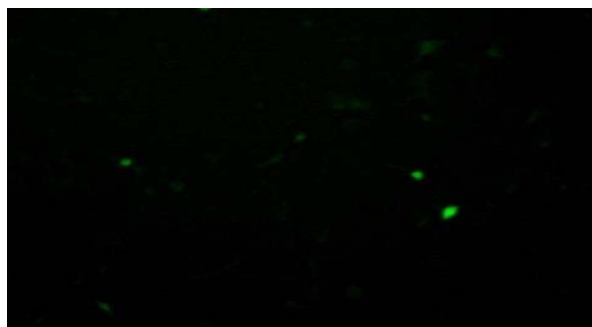
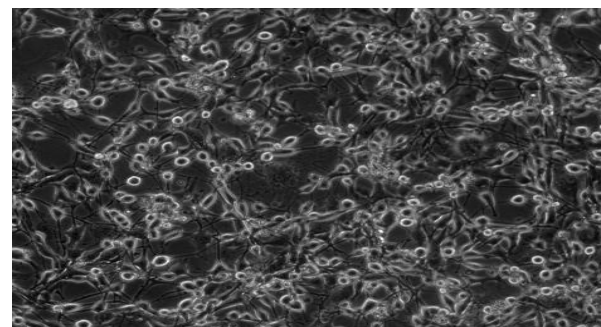


Fig 6

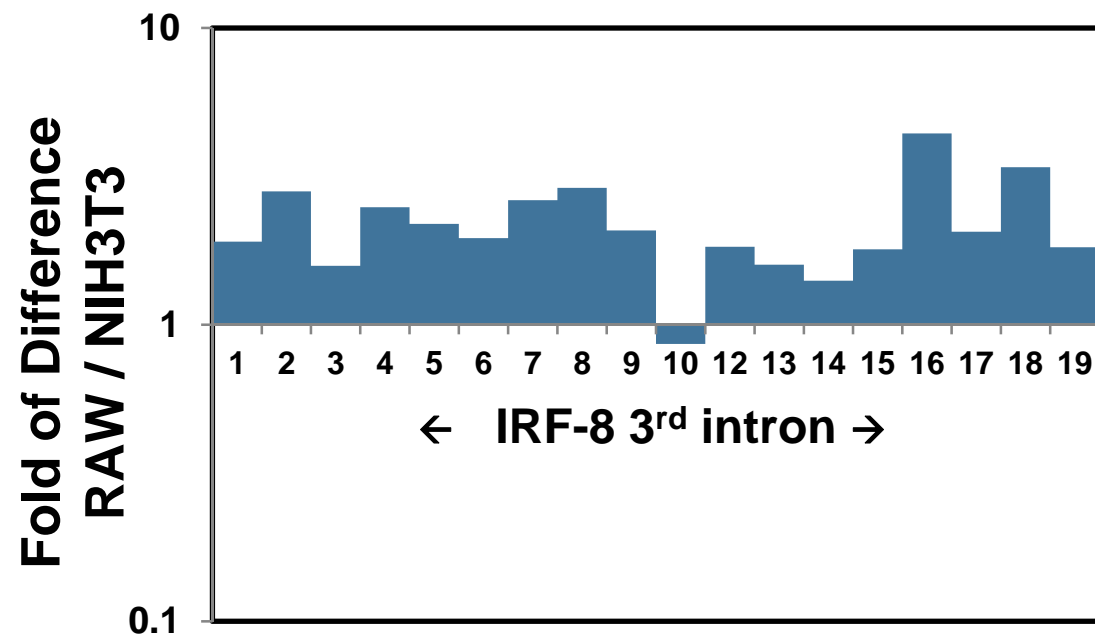
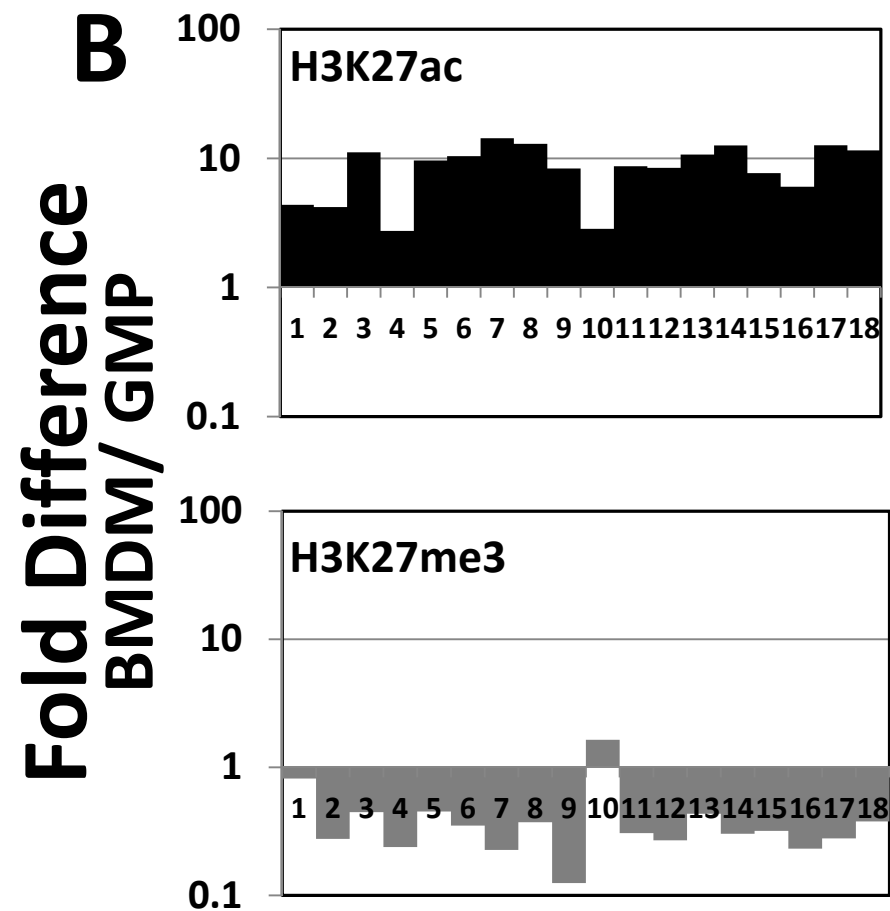
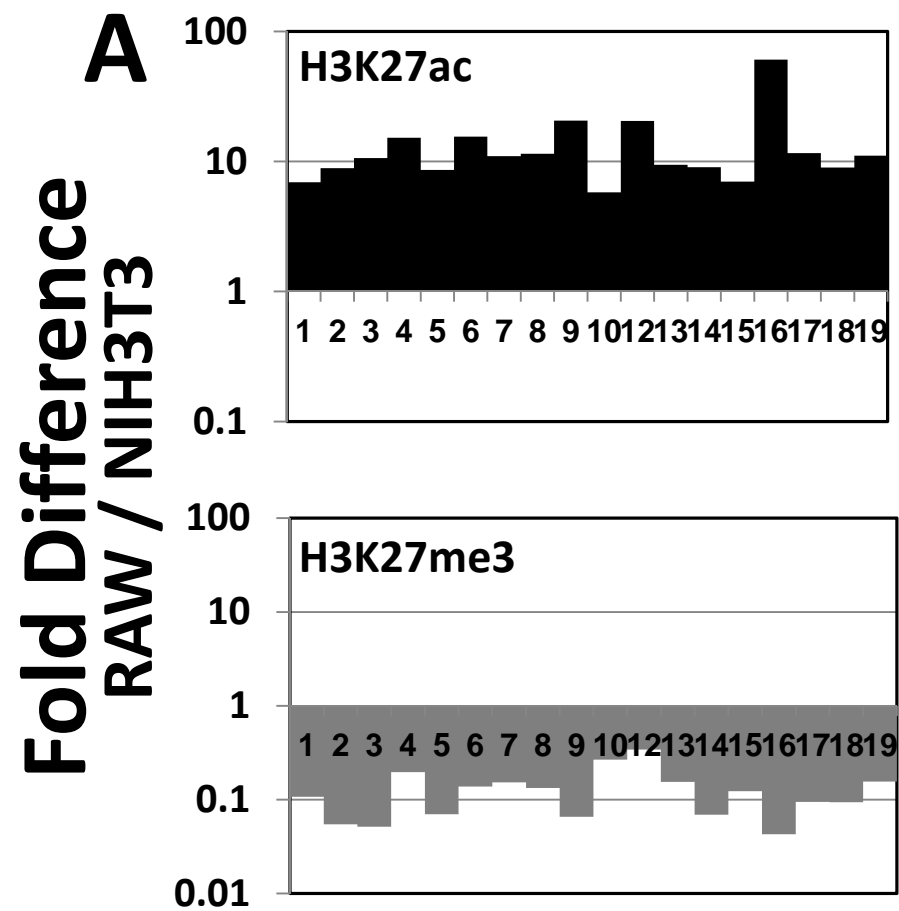
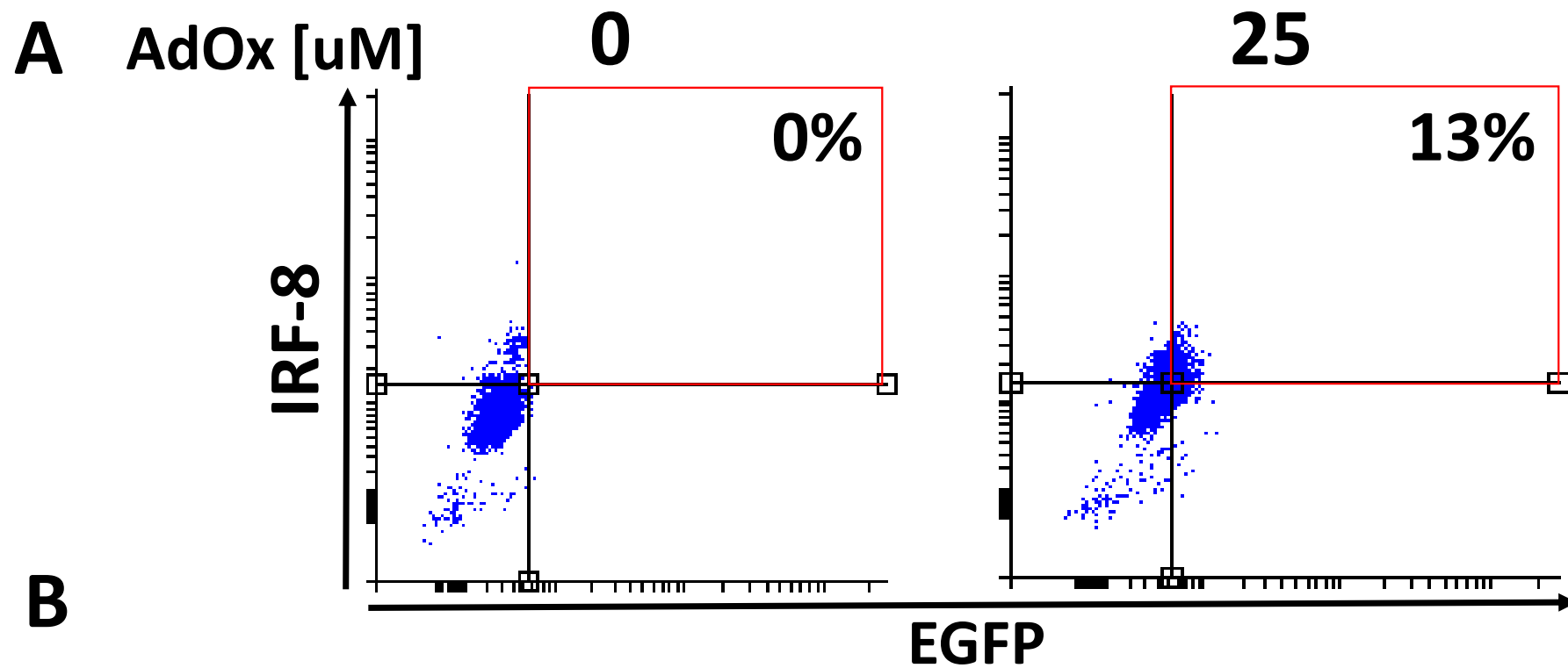


Fig 7





B

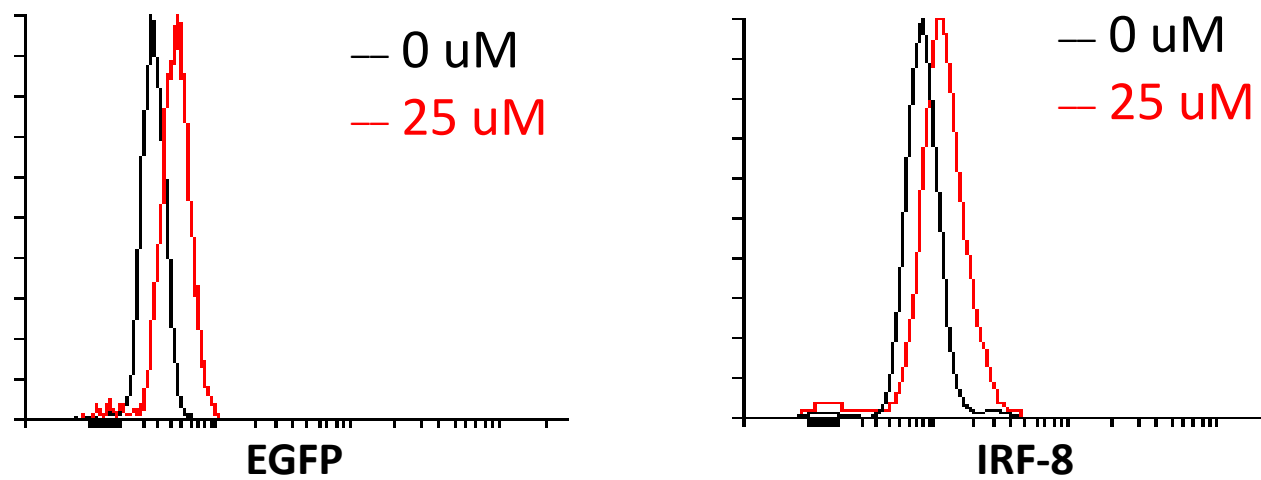
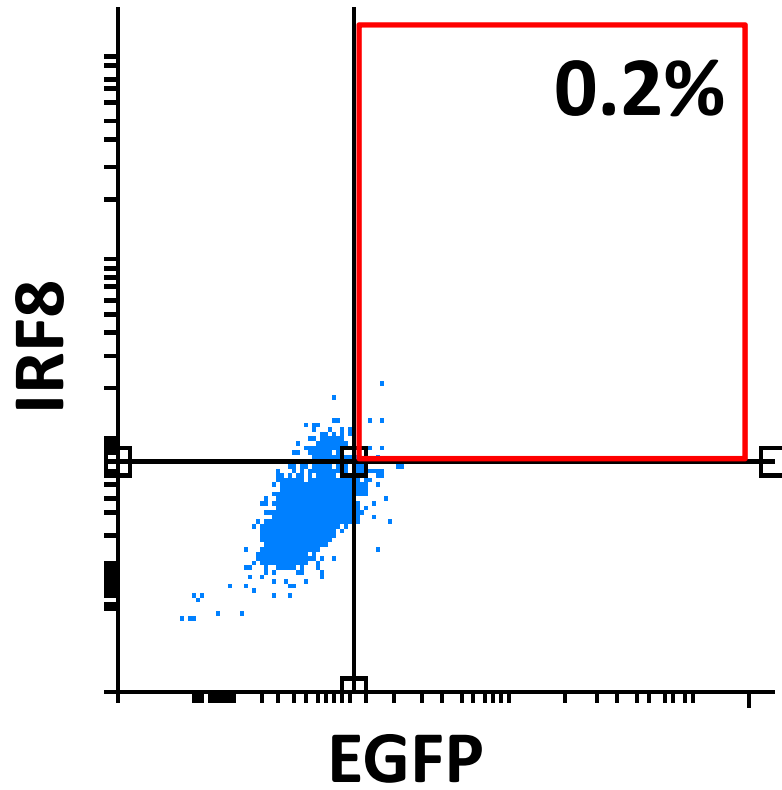


Fig 8

3T3-IRF8.1



3T3-IRF8.1+shRNA_Mafk

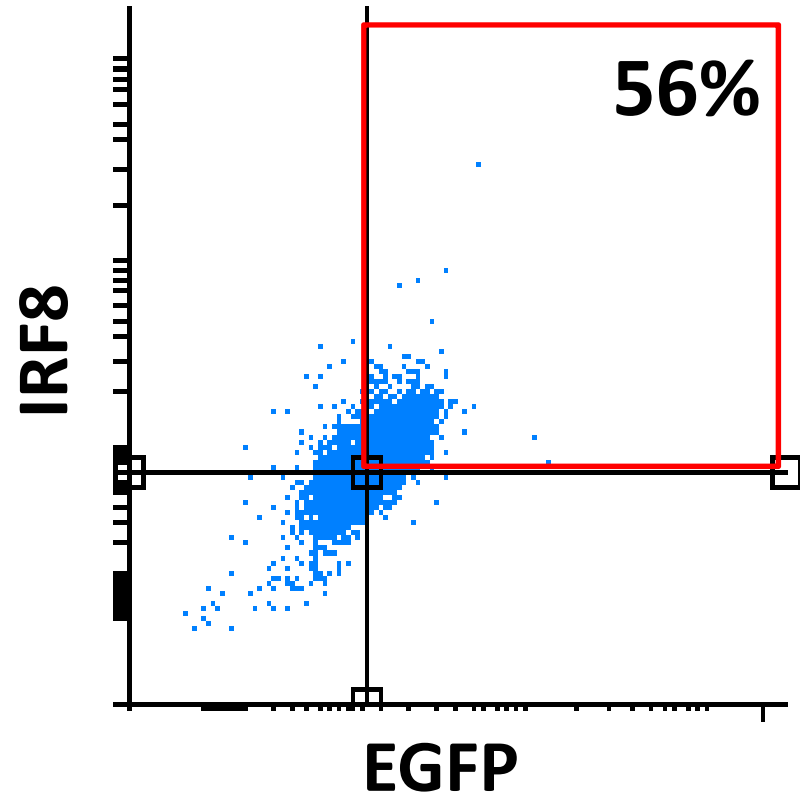


Fig 10

Fig 1S

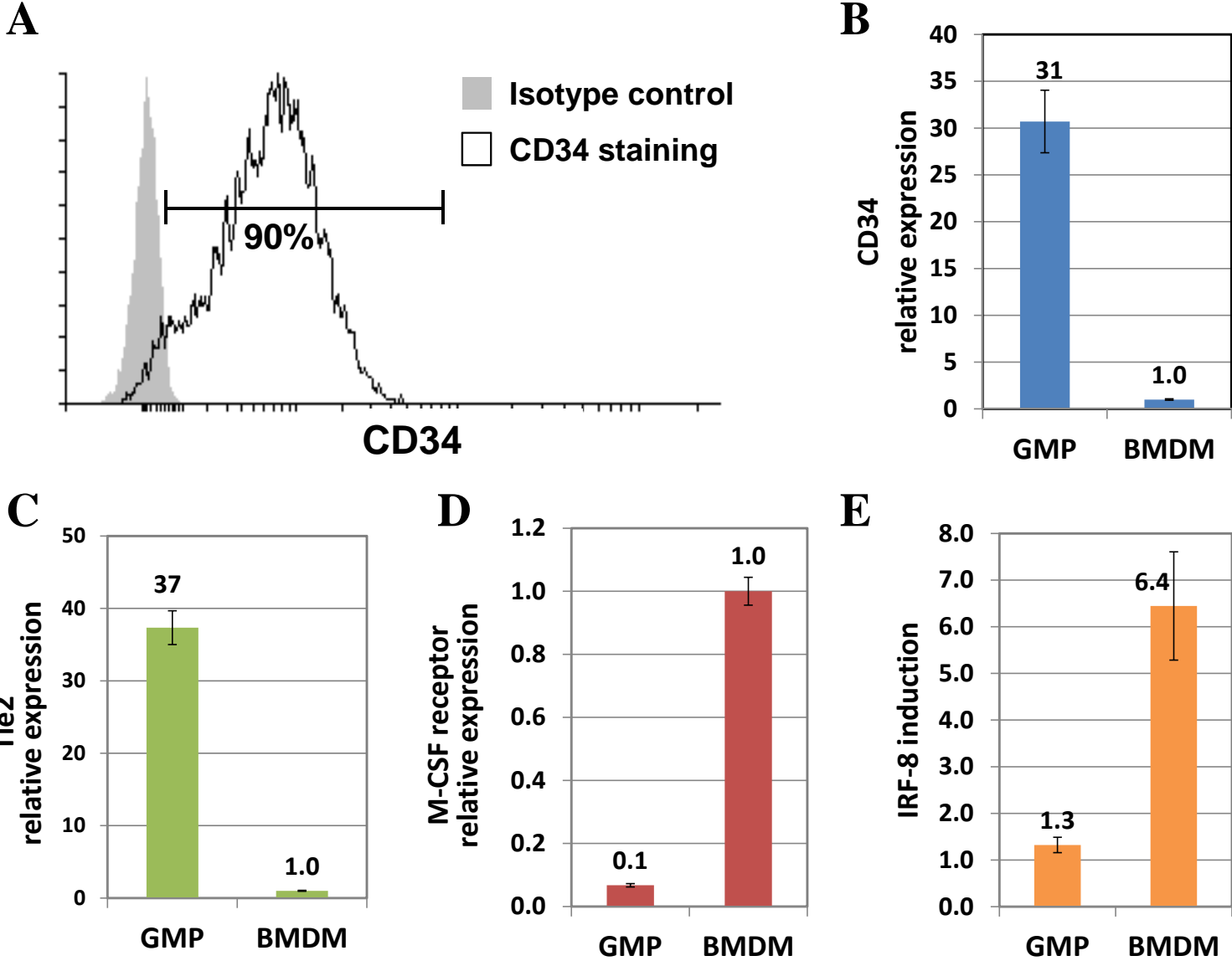


Fig 2S

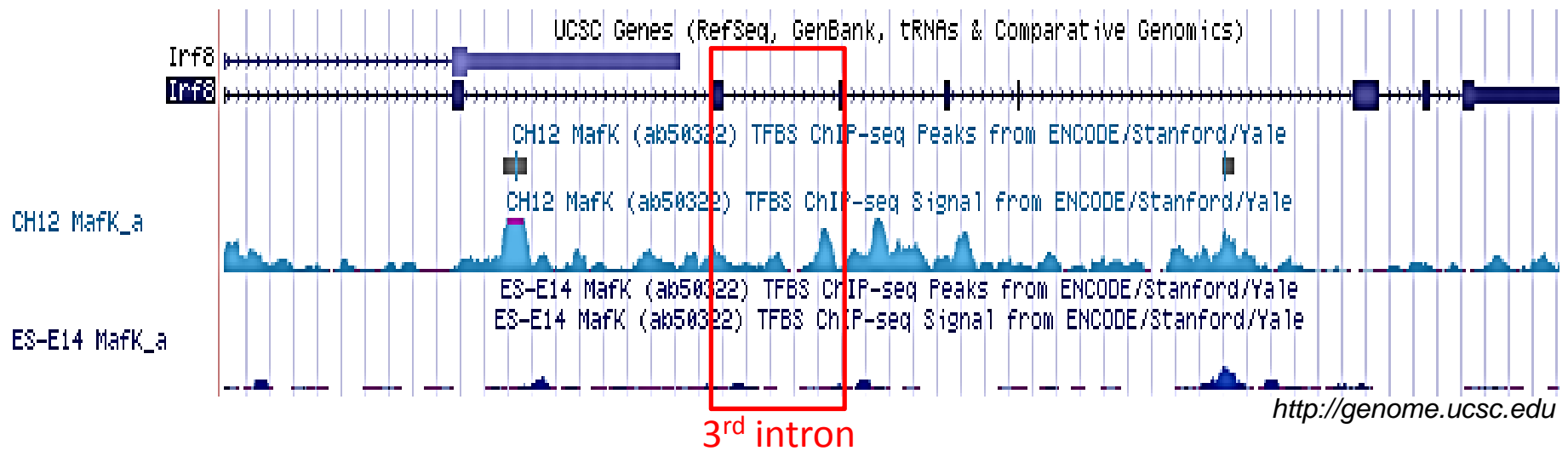


Fig. S3

